HHS Public Access

Author manuscript

Res Math Sci. Author manuscript; available in PMC 2021 December 01.

Published in final edited form as:

Res Math Sci. 2020 December ; 7(4): . doi:10.1007/s40687-020-00230-7.

Effective behavior of cooperative and nonidentical molecular motors

Joseph J. Klobusicky,
The University of Scranton, Department of Mathematics, Scranton, PA, USA

John Fricks,
Arizona State University, School of Mathematical and Statistical Sciences, Tempe, AZ, USA

Peter R. Kramer
Rensselaer Polytechnic Institute, Mathematical Science Department, Troy, NY, USA

Abstract

Analytical formulas for effective drift, diffusivity, run times, and run lengths are derived for an intracellular transport system consisting of a cargo attached to two cooperative but not identical molecular motors (for example, kinesin-1 and kinesin-2) which can each attach and detach from a microtubule. The dynamics of the motor and cargo in each phase are governed by stochastic differential equations, and the switching rates depend on the spatial configuration of the motor and cargo. This system is analyzed in a limit where the detached motors have faster dynamics than the cargo, which in turn has faster dynamics than the attached motors. The attachment and detachment rates are also taken to be slow relative to the spatial dynamics. Through an application of iterated stochastic averaging to this system, and the use of renewal-reward theory to stitch together the progress within each switching phase, we obtain explicit analytical expressions for the effective drift, diffusivity, and processivity of the motor-cargo system. Our approach accounts in particular for jumps in motor-cargo position that occur during attachment and detachment events, as the cargo tracking variable makes a rapid adjustment due to the averaged fast scales. The asymptotic formulas are in generally good agreement with direct stochastic simulations of the detailed model based on experimental parameters for various pairings of kinesin-1 and kinesin-2 under assisting, hindering, or no load.

Keywords

Molecular motors; Stochastic averaging; Switched diffusion; Renewal-reward theory

corresponding author The University of Scranton, Department of Mathematics, Scranton, PA, USA, joseph.klobusicky@scranton.edu.
Dedicated to Andy Majda for his 70th birthday, with gratitude for his lasting inspiration starting from my undergraduate and graduate days on the creative deployment of mathematical modeling and the beautiful application of analysis techniques as a lens for exploring and understanding the dynamics of physical systems - PRK

Conflicts of interest/Competing interests
The authors declare no conflicts of interest.

Code availability (software application or custom code)
Code was developed simply to simulate the model to check the theory. As no novel computational methodology was involved, we do not view the code to be of sufficient general interest to publish it.

1 Introduction

A biological cell during its interphase requires sufficiently fast transport of organelles and other compounds for its survival [1]. Transport through diffusion alone is often far too slow. To illustrate, a compound moving through pure diffusion in some neurons might take years to travel over the cell's length [2]. For eukaryotic organisms, intracellular trafficking of vesicles is instead governed by directed transport along a network of thin filaments, such as microtubules or actin. A vesicle and the molecular compound it encloses, collectively referred to as a cargo, travel along the filaments by attaching to one or several molecular motors. As an important example on which we will focus, we can consider molecular motors called kinesins, which consist of two heads which attach to a microtubule, a tail which attaches to the cargo, and a coiled-coil tether connecting the heads and tail [3]. But the mathematical framework to be developed can be applied to more general molecular motors, including dynein and myosin.

The motor-cargo attachment is generally found to be much more durable than the motor-microtubule attachment [4], so models of motor-cargo complexes typically assume the number of motors attached to a given cargo can be treated as a fixed constant N over the transport time scale of interest [5-9]. But the number of those N motors that are attached to microtubules and therefore actively engaged in transport does appear to fluctuate through dynamical attachment and detachment of the motors to and from the microtubule. In the present work, we contemplate the simplest scenario in which the motor-cargo complex is in the vicinity of a single microtubule. The state of the motor-cargo complex can then be classified in terms of which of its motors are attached to the microtubule, and therefore engaged in directed motion. Our model could also be formally applicable for a bundle of parallel microtubules with common polarity if they are spaced sufficiently closely that the progress of the cargo is not so sensitive to what particular set of microtubules the motors are attached. Experimental observations [10, Fig. S5] show that approximating the multiple motors as all attached to a single microtubule could be consistent even for some situations in cell.

A cargo with two motors, for example, can fluctuate between three possible states while remaining connected to the microtubule: two states with one attached and one detached motor, and one state with two attached motors (Figure 1). One further state has both motors detached, after which we will consider the cargo to move away from the microtubule and terminate its run, though one could contemplate the motors remaining weakly bound and possibly sliding along the microtubule [11, 7].

Microtubules are oriented with a + and − end, with the molecular motor kinesin always traveling from the − to + end [1] and the molecular motor dynein traveling in the opposite direction. This can result in "tug of war" scenarios and bidirectional transport for ensembles including such antagonistic motors [12]. Our focus here is on cooperative transport of a cargo by possibly different motor types which each move, when considered in a single motor complex, in the same direction on the microtubule, such as two different types of motors from the kinesin superfamily. Since we wish to contemplate the possibility of the motors being of different types, motor labelling is relevant and we distinguish between the two

states with one motor attached. This is in contrast to models with N identical motors attached, which can be classified more compactly in terms of simply the number of those motors which are currently attached to a microtubule [13]. For multiple motor complexes, we are interested in calculating how statistics such as run lengths and effective speeds depend on the properties of the individual motors. Comparisons of statistics between motor complexes are not always intuitive. For instance, it has been observed in [14] that heterogeneous motor complexes of kinesin-1 and kinesin-2 have longer run lengths than pure systems consisting only of kinesin-1. This observation would seem to depend upon a variety of physical parameters, often interacting in complex ways. Indeed, while kinesin-2 is about half as fast as kinesin-1 and detaches more readily under load, it also appears to reattach to microtubules four times more quickly than kinesin-1 [14].

A number of properties of some individual motors, acting in isolation, have been obtained from in vitro experiments with optical traps, in which a polystyrene bead, serving as a cargo, is attached to a motor, and directed along a microtubule with an applied optical trap force. Under this setting, several motor properties can be measured, particularly their speed, diffusivity, and detachment rate as a function of the applied optical trap force [15-21]. The above experimental work can be used as a basis for parameterizing biophysically mechanistic models for individual motors in theoretical models exploring their interactions [6, 22-31]. For the purpose of experimentally measuring the interaction of molecular motors, and in particular for motivation for and comparison against theoretical models, an important experimental development has been to use DNA origami for cargo, which specifies closely arranged handle sites onto which specified motor types attach [14, 27, 32]. The actual engagement of motors with microtubules cannot be resolved, so particularly when not using engineered motor-attachment constructs, the number of relevant motors of various types attached to an observed cargo with a particular microtubule must typically be statistically inferred, sometimes using simple theoretical models [10, 33, 9].

1.1 Overview of Methods and Results

Our mathematical modeling framework is based on the one developed in McKinley, Athreya, et al [34], where cargo transport statistics were examined for cooperative ensembles of identical motors that are treated as permanently attached to the microtubule. The coupled spatial dynamics of the motor and cargo position are expressed as a system of continuous stochastic differential equations (SDEs) which are viewed as a coarse-graining of discrete stepping model. The model is posed in essentially one spatial dimension along the microtubule, neglecting transverse fluctuations. We extend the model in [34] in two ways: 1) allowing the motors to be distinct, but still cooperative, and 2) allowing the motors to attach and detach from the microtubule. This model represents the motor-cargo system in terms of basic parameters concerning biophysical properties of the individual motors and the cargo. The cargo and detached motor dynamics are modeled as overdamped point particles responding to spring forces from the motor-cargo tether and driven by stochastic terms representing thermal fluctuations. On the other hand, as in [34], the attached motors dynamics are governed by a nonlinear force-velocity relation together with stochastic terms arising from the nonequilibrium stepping process. Punctuating the continuous evolution of the motor-cargo dynamics is the attachment or detachment of motors from the microtubule.

These are represented in terms of Markovian jump processes, with attachments occurring at constant rates but the detachments occurring at rates dependent upon the force on the motor.

To characterize the effective behavior of the motor-cargo complex as a whole, we proceed through a sequence of coarse-graining steps motivated by the separation of time scales of the various physical processes. First we average over the fast dynamics of the cargo and detached motors. This can be accomplished easily for arbitrary number N of cooperative motors, but our further analytical progress is restricted to the case of $N = 2$ cooperative motors due to the substantial increase in complexity for $N > 2$. We homogenize over the spatial dynamics of the attached motors between attachment and detachment events. This eventually yields an effective Markov chain description in terms of jumps between different states of motor attachment, with associated durations and displacements of the motor-cargo complex within each state. By decomposing the stochastic trajectory through this finite state space in terms of cycles demarcated by moments when both motors are attached, we further coarse-grain the motor-cargo dynamics into a renewal-reward process. With Wald's identity, we characterize the fundamental statistics of the run length and run time of the motor-cargo complex in terms of the statistics of duration and displacement over one of these cycles, which are in turn related to the basic biophysical parameters of the model. With a law of large numbers argument and its application to renewal-reward processes, we relate the effective velocity and diffusivity also to the cycle statistics, and thereby in turn to the basic biophysical parameters. We next proceed to discuss the components of our analysis in some more detail, with reference to related work.

1.2 Modeling approach

The reason we work with the coarse-grained SDE model for the motors is to reduce the number of physical parameters modeling the individual motor to those characterizing the force-velocity relationship, the force-detachment relationship, and a noise parameter. Moreover, the mathematical presentation is simplified by having the cargo and motor dynamics in a unified SDE framework. One could of course start with a motor stepping model [26, 35-37, 5, 38, 39, 30, 25], and readily coarse-grain it to obtain the parameters for our SDE model, and the conclusions would be equivalent unless the cargo fluctuations fed back on the force-dependent kinetics of stepping in a substantially different way than they do on the force-dependent coarse-grained velocity. We cannot rule such subtle feedback out [40], but if it were real, one would presumably have to represent the chemomechanical stepping cycle in more detail to capture these effects than a generic stepping model with one step per cycle. The detailed description of the stepping dynamics of even well-studied motors such as kinesin-1 is still under active experimental investigation [18, 41, 16], while the more coarse-grained characterizations needed for the SDE description are more consistently established across labs. For these reasons, we will proceed here with the coarse-grained SDE description, in somewhat the same vein as coarse-grained integrate-and-fire models are often used in place of more detailed Hodgkin-Huxley models to study networks of interacting neurons [42-49].

In Section 2, we present our extended model allowing for distinct motors and attachment/detachment from the microtubule. The modification of the spatial dynamics is presented in

Subsection 2.1, resulting in a system of SDEs (1)-(4) with the motor dynamics depending on both the motor label and whether the motor is attached or detached. In Subsection 2.2, we present our model of switching times. Attachment rates are rather difficult to quantify experimentally and appears to depend on the operating conditions and whether the motor is tethered near the microtubule by other motors [27, 32, 50], and we simply adopt the common approach of modeling them as constant (as in a homogenous Poisson process model). The detachment rates, on the other hand, will be taken as functions of the applied force on the attached motor, which is itself a stochastic process induced by the stochastic spatial dynamics. Mathematically, then, the detachment process is more akin to a Cox process [51, 52]. The class of functions we consider for detachment rates is general enough to include the most common cases seen in previous works, including constant [53], exponential [18, 22, 54, 13], double-exponential functions [17], and exponential functions turning over to slower linear growth beyond stall [6, 55] or along the assisting direction [56].

Transitions between attached and detached states have been modeled as continuous time Markov chains in the case of identical motors [13, 57, 58, 24] with constant switching rates depending on the number of attached and detached motors. Our model allows for nonidentical motors, which increases the state space of possible attachment and detachment configurations. Similar to the discrete-space models discussed in [57, 58], our transition rates depend on relative motor positions, but now must consider motor types. Moreover, our model does not make the popular assumption [13, 24, 27] that the cargo is always in mechanical equilibrium with the motors nor the further mean-field approximation that all motors feel a perfectly shared load from the cargo. Stochastic fluctuations of cargo and motor positions have been shown to significantly alter the mean-field predictions, at least for small teams of motors [22, 59, 6], and experimental observations do not support the load-sharing assumption in teams of two kinesin-1 [27]. Bouzat [26] shows how the neglect of fluctuations in the cargo position can give incorrect modeling results for the effective force-velocity response of a single motor and in particular for the stall force of cooperative motors. Berger, Müller, and Lipowsky [60] and Arpağ, Norris, et al [56] similarly find the force felt by a motor from the cargo substantially affects its effective detachment rate, and so departs from the mean-field dynamical description by averaging the detachment rate against the modeled probability distribution of the force applied by the cargo in a given configuration of attached and detached motors. We apply a similar, but more systematic, procedure in Subsection 4.3.1 to compute effective detachment rates by averaging over a quasi-stationary distribution of the force felt from the cargo, as a function of the current configuration of attached motors. Uppulury, Efremov, et al [59] and Kunwar, Tripathy, et al [6] conducted informative simulation studies of discrete-state stochastic stepping models that keep track of the relative positions of identical motors, but did not develop analytical formulas relating collective behavior to single-motor properties. Keller, Berger, et al [25] similarly conducted simulation studies for a pair of identical motors which resolved the chemomechanical steps, finding in particular that the transport is degraded as the strength of the Hookean tether coupling the motors and cargo is increased. Wang and Li [5] derive an analytical formula for the effective velocity of a cooperative team of identical stochastic stepping motors, but don’t include attachment and detachment effects. Li, Lipowsky, and Kierfeld [61] developed a variation of the Markov chain model of Klumpp and Lipowsky [13] for cooperation by two

groups of motors, one fast and one slow, in the context of gliding assays where the numbers of engaged motors are considerably larger than for cargo transport, to relate bistability in the transport of microtubules to a small ratio of detachment force scales to the stall forces. A recent model by Miles, Lawley, and Keener [31] for cooperative molecular motor transport employs a similar framework to ours, with a stochastic differential equation for the cargo dynamics, but with step-resolving dynamics for the motors. The model we present extends the model of [31] in allowing the motors to be nonidentical and allowing the detachment rates of motors to depend on the spatial configuration of the motors.

1.3 Computation of transport statistics

The analysis of our model will proceed in Section 3 by an extension of the asymptotic analysis developed in McKinley, Athreya, et al [34], based on the cargo dynamics being taken as fast relative to the dynamics of the motors attached to the microtubule. Extending this nondimensionalization to our setting of nonidentical motors which attach and detach from the microtubule in Section 3.1, we further motivate taking the detached motor dynamics to be faster than the cargo (due to their relative size), and the attachment and detachment processes as slow compared to the dynamical time scale of attached motors. A similar hierarchy of time scales was considered in the context of the stepping of the two heads of a kinesin motor attached to a cargo in Peskin and Oster [62], where the detached head was taken to move quickly relative to the cargo, while the cargo dynamics were taken as fast relative to the time scale of motor stepping.

We set up an asymptotic analysis which formalizes the separation of time scales we identify, with the further assumption that the parameters for different motor types do not vary drastically (which seems to be reasonable for kinesin-1 versus kinesin-2, for example, [18]). We proceed in Subsection 3.2 to apply stochastic averaging successively over the unbound motor positions and the cargo position to obtain effective dynamics and effective detachment rates based only on the positions and identities of the attached motors. The analysis thus far applies to N cooperative but possibly not identical motors, and in fact does not require a time scale separation assumption between the attached motor dynamics and attachment/detachment dynamics. In Section 4, we use this scale separation assumption for the case of $N = 2$ motors to proceed further by homogenizing the effective dynamics obtained from the stochastically averaged equations within each interval between attachment or detachment, and averaging the detachment rates over the spatial configurations of the motor-cargo complex.

Finally, in Section 5 we develop theoretical formulas for the effective velocity, diffusivity, and processivity statistics of the motor-cargo complex, all expressed in terms of explicit formulas involving the parameters governing the motor and cargo dynamics. The appropriate definition of velocity and diffusivity requires some consideration when applied to random finite time intervals over which the cargo remains associated to a microtubule, and we consider two versions relevant to different protocols of computational simulation or experimental observations where data from multiple runs are collected. Our method of deriving these effective transport statistics is through the application of the law of large numbers and renewal-reward asymptotics to the progress made by the motor-cargo complex

over several cycles of attachment and detachment events. Krishnan and Epureanu [63] developed some early ideas for how to interpret experimental statistics for molecular motor systems using results from renewal-reward theory. Hughes, Hancock, and Fricks [37] appealed to renewal theory arguments for a discrete semi-Markov stepping model to compute effective statistics for motor head stepping from a chemomechanical cycle model, and Shtylla and Keener [64] applied this framework to describe the effective dynamics of a ParB protein complex that moves along a track of ParA proteins in a manner similar to molecular motors which "burn" the track as they progress. In a broad sense, our strategy of combining asymptotic arguments regarding separation of time scales and renewal-reward calculations to obtain these explicit formulas mirrors that of Miles, Lawley, and Keener [31] for the case of identical cooperative motors with force-independent detachment rates, though our implementation of these ideas differ in some details which we will discuss in the conclusion (Section 7).

We show in Section 6 that our theoretical formulas obtained by these scale separation arguments for the effective transport of kinesin-1/kinesin-1, kinesin-2/kinesin-2, and kinesin-1/kinesin-2 complexes compare generally well with direct numerical simulations of our model as parameterized by experimental observations of individual kinesin-1 and kinesin-2 motors. A few issues in translating experimental observations into model parameterization, however, require study before our predictions based on our mathematical framework can meaningfully be compared directly with experimental observations [14, 27] of pair complexes of kinesin-1 and kinesin-2. Our objective in the present work is on the development of the general mathematical coarse-graining procedure and formulas for cooperative molecular motor transport in terms of the biophysical properties of the constituent motors, and we provide in Section 7 an assessment of the merits of this mathematical approach as well as limitations whose resolution will motivate future work.

2 Models of evolution and switching

For a fixed number of attached and detached motors, we model the transport of a motor and cargo system through a system of SDEs. Similar to McKinley, Athreya, et al [34], we coarse-grain over this discrete stepping and model this motion as a one-dimensional continuous process along the direction of the microtubule, neglecting transverse fluctuations which might not be so significant [30]. The locations of N motors over time t are denoted by $X^{(i)}(t) \in (-\infty, \infty)$, $i = 1, \ldots, N$. All motors in the system are assumed to remain attached to a single cargo, with a position of $Z(t) \in (-\infty, \infty)$. During a realization of the stochastic process, a motor will change its state from time to time. We will denote the ith motor's state at time t as $Q^{(i)}(t) \in \{0, 1\}$, where 0 and 1 denote states of detachment or attachment to the microtubule, respectively. The switching between motor states will be governed by a jump process, which is Markovian with respect to the filtration generated jointly by $\{X^{(i)}(t)\}_{i=1}^{N}$, $Z(t)$ and $\{Q^{(i)}(t)\}_{i=1}^{N}$, and with switching (jump) rates due to attachment and detachment depending on the spatial displacements between the motors and cargo.

2.1 Drift and diffusion of nonidentical motors

For a motor system with N motors the governing equations take, for $i = 1, \dots, N$, the autonomous form

$$\begin{aligned} dX^{(i)}(t) = &\left(\boldsymbol{\mu}_d^{(i)}(X^{(i)}(t), Z(t))dt + \sqrt{2k_BT / \boldsymbol{\gamma}_m^{(i)}}dW^{(i)}(t)\right)(1 - Q^{(i)}(t)) \\ &+ \left(\boldsymbol{\mu}_a^{(i)}(X^{(i)}(t), Z(t))dt + \boldsymbol{\sigma}^{(i)}dW^{(i)}(t)\right)Q^{(i)}(t), \end{aligned} \tag{1}$$

$$\boldsymbol{\gamma}dZ(t) = \sum_{j=1}^{N} F^{(j)}(X^{(j)}(t) - Z(t))dt - F_T dt + \sqrt{2k_BT\boldsymbol{\gamma}}dW_z(t)\,. \tag{2}$$

with drift coefficients $\mu_a^{(i)}$, $\mu_d^{(i)} : \mathbb{R}^2 \to \mathbb{R}$ for the motors satisfying

$$\boldsymbol{\mu}_a^{(i)}(x, z) = v^{(i)}g(F^{(i)}(x - z) / F_s^{(i)}), \tag{3}$$

$$\boldsymbol{\mu}_d^{(i)}(x, z) = -F^{(i)}(x - z) / \boldsymbol{\gamma}_m^{(i)}\,. \tag{4}$$

A table of the parameters and their roles can be found in Table 1. We next briefly summarize the meaning of the model equations (1)-(4); more details can be found in [34].

If $Q^{(i)}(t) = 1$, equation (1) describes an attached motor with position $X^{(i)}(t)$. The restorative force in (3) results from the stretching of the coiled-coil tether that connects the motor head and tail attached to the cargo. While a nonlinear force model for the tether would seem to be most appropriate [27, 59, 65], we could not find a clear consensus on its precise form. To reduce technical complications in the formulas and to keep focus on the overall structure of the mathematical course-graining, in the present work, similarly to Miles, Lawley, and Keener [31], we model the force for this tether for motor i by a simple Hookean spring relation $F^{(i)}(y) = \boldsymbol{\kappa}^{(i)}y$, where y is the longitudinal displacement from the cargo to the motor, and $\boldsymbol{\kappa}^{(i)}$ is the effective spring constant for the tether to the ith motor. The value we have cited from Furuta, Furuta, et al [32] is measured from motors attached to a DNA scaffold, but we expect the stiffness to mostly reflect the properties of the motor tether [30]. The value is roughly consistent with the $\boldsymbol{\kappa} \approx 0.3$ pN/nm values found in other experiments [66, 54, 65]. Surely a better model for the tether would have it be slack under compression from its rest length [54, 67, 56, 68, 32]. While we do not investigate the consequences of nonlinear tether force models here in detail, our framework can be generalized to include them, as discussed in Appendix A.

The nondimensional force velocity relation $g : \mathbb{R} \to \mathbb{R}$ is multiplied by an unencumbered velocity $v^{(i)}$ to produce an instantaneous expected velocity. The argument of g measures the ratio between the tether force and the motor's stall force $F_s^{(i)}$, or the opposing force needed from the cargo to anchor a motor. Positive arguments of g correspond to forces opposing or hindering the free motion of the motor. To agree with the definitions of $v^{(i)}$ and $F_s^{(i)}$, g must satisfy $g(0) = 1$ and $g(1) = 0$. Random effects are modelled by independent Brownian

motions $W^{(i)}(t)$, with an effective motor diffusion of $\frac{1}{2}(\sigma^{(i)})^2$. In Table 1, we have used randomness parameters for kinesin 1 and 2 found in [69, 18] to calculate diffusivities via their relation which can, for example, be found in Eqn. (47) of Krishnan and Epureanu [63].

When $Q^{(i)}(t) = 0$, the equation for the position of an detached motor $X^{(i)}(t)$ in (1) is an overdamped Langevin equation for a particle with a friction constant $\gamma_m^{(i)}$, and spring constant $\kappa^{(i)}$. The friction constant $\gamma_m^{(i)}$ was computed with the Stokes-Einstein relation $\gamma_m^{(i)} = 6\pi a\eta$ for a spherical object with radius $a = 50$ nm in water, with a fluid dynamic viscosity of $\eta = 10^{-9}$ pN s/nm^2. The Brownian motions $W^{(i)}(t)$ are independent of each other, and also of the Brownian motion $W_Z(t)$ driving the cargo. Finally, the constant k_BT is the Boltzmann constant multiplied by temperature.

The equation for cargo position $Z(t)$ in (2) also follows an overdamped Langevin equation with friction constant γ (also calculated using the Stokes-Einstein law with $a = 500$ nm), but differs from that of detached motors in two ways. First, the cargo is subject to spring forces from each of the N motors. Second, we also account for a possible constant applied optical trap force F_T, as in the experiments of [6, 17, 16] and simulations of [26, 40, 13, 22, 67, 27]. Note that the friction constant values for the detached motors and cargo should be viewed in a somewhat notional sense, and we have not attempted to give them precise values. Fortunately as will discuss in Section 7, the effective dynamics are not sensitive to their precise values.

2.2 Switching between attachment configurations

We model the transition between attachment configurations with varying numbers of attached and detached motors with jump processes. See Table 1 for a list of typical attachment/detachment values. The attachment of motors is modeled by a homogeneous Poisson process, with each detached motor having an attachment rate of $a^{(i)}$. As in most theoretical work [13, 6, 26], we take the attachment rates to be independent of the configuration of the motor-cargo complex, though we acknowledge that Furuta, Furuta, et al [32] finds significant reduction of the attachment rate of a second motor when the cargo is under load. The attachment rate of a motor can naturally be expected to be somewhat different when at least one other motor on the same cargo is also attached to a microtubule than when none are [31], as does seem to be indicated experimentally [27]. As we do not model the attachment of the motor-cargo complex from a state of no attached motors, the attachment rate we require is the one where at least one other motor on the same cargo is currently attached to a microtubule. We therefore take our parameter value for $a^{(i)}$ in Table 1 from recent experimental measurements in this setting [14], rather than the conventional estimate in modeling work [13] based on single-kinesin attachment rates. When a motor reattaches, we simply place it at the same position along the microtubule as it was previously in the detached state.

This is a bit different than most other reattachment models in the literature, which do not precisely track the motor position in the detached state (as we do), but apply a selection rule of where the motor reattaches. For example, [25] attaches the second motor at a location that leads to a zero tether force with the cargo, while [31] attaches the motor directly at the

current cargo position. By contrast, [32, 26, 67, 68] randomly choose attachment sites that are within a geometrically defined range of the motor's attachment point to the cargo while [9, 30] preferentially reattaches a motor to the microtubule at locations that require the least strain energy on the motor. Our approach, as well as the other random models just cited, are consistent with experimental observations that a motor can reattach ahead or behind the motor already attached [14].

Detachment rates are determined through the function depending on the force F felt by the motor:

$$d^{(i)}(F) = d_0^{(i)} \Upsilon^{(i)}(F \,/\, F_d^{(i)}) \,. \tag{5}$$

Here, the parameter $F_d^{(i)}$ is a scale force, and $\Upsilon^{(i)}$ satisfies $\Upsilon(0) = 1$, so that $d_0^{(i)}$ is the detachment rate under no external force. Note that since we are only modeling the motor-cargo dynamics along the microtubule direction, our detachment rate model correspondingly depends only on the longitudinal force F, with a positive sign corresponding to opposing the motor's natural direction of motion. Note this convention of writing the relation of the detachment rate and applied force with positive arguments corresponding to a hindering force is opposite to how such relations are typically presented in recent experimental studies [16, 17, 70] but are consistent with how force-velocity relationships are typically expressed in theoretical and simulation studies [24, 26, 34]. The force $F = F^{(i)}(t)$ opposing the motor i at time t consists of the force from the tether to the cargo, which is

$$F^{(i)}(t) = \boldsymbol{\kappa}^{(i)}(X^{(i)}(t) - Z(t)) \,. \tag{6}$$

As $F^{(i)}(t)$ is a random process, so is the detachment rate $d^{(i)}(F^{(i)}(t))$ of motor i. The resulting model for detachment thus amounts to a Cox process, a generalization of a Poisson process in which the intensity function may be a random process (see Cox and Isham [51] for an introduction).

We can formalize the description of the switching model through the association of standard Poisson counting processes with each potential state transition. We thereby define, with associations, the standard Poisson counting processes $Y_{\mathrm{d}}^{(i)}(t)$ to represent detachment of motor i and $Y_{\mathrm{a}}^{(i)}(t)$ to represent attachment of motor i. Then the dynamics of the attachment states can be written, for $i = 1, \ldots, N$:

$$\begin{aligned} dQ^{(i)}(t) = {} & Y_{\mathrm{a}}^{(i)}\left(a^{(i)} \int_0^t (1 - Q^{(i)}(t'))dt'\right) \\ & - Y_{\mathrm{d}}^{(i)}\left(\int_0^t Q^{(i)}(t') d_0^{(i)} \Upsilon^{(i)}\left(\boldsymbol{\kappa}^{(i)}(X^{(i)}(t') - Z(t')) \,/\, F_d^{(i)}\right)dt'\right). \end{aligned} \tag{7}$$

Together with Eqs. (1)-(4) from Subsection 2.1, we have a complete Markovian dynamical description for the motor-cargo model.

A common choice of $\Upsilon^{(i)}$, following the theory of Bell [71], is an exponential function (see [7, 22], for instance). For simulations in Section 6, we will use the more general double exponential detachment model, which is based on observations that run length is asymmetric with respect to the direction of external load [16, 17], which can be argued to improve the processivity of a team of motors [67]. Detachment rates for the double exponential detachment model are given by

$$d^{(i)}(F) = \begin{cases} d_{0-}^{(i)} \exp(-F / F_{d-}^{(i)}) & F \leq 0, \\ d_{0+}^{(i)} \exp(F / F_{d+}^{(i)}) & F > 0. \end{cases} \tag{8}$$

Here, $d_{0+}^{(i)}$ and $d_{0-}^{(i)}$ are, respectively, limits of detachment rates as the hindering (assisting) external force approaches zero. The corresponding force scales $F_{d+}^{(i)}$ and $F_{d-}^{(i)}$ of detachment are expressed in the literature [16, 17] in terms of characteristic length scales $\boldsymbol{\delta}_{+}^{(i)}$ and $\boldsymbol{\delta}_{-}^{(i)}$ via $F_{d\pm}^{(i)} = k_B T / \boldsymbol{\delta}^{(i)}$. Note again our sign convention on the force is opposite to how the experimental results are presented in [16, 17], but is consistent with the standard representation of force-velocity relations in theoretical studies. In our one-dimensional model, we are not distinguishing between longitudinal and transverse force components, which may have interesting dynamics from geometric considerations of the cargo [27].

From the additivity of Poisson rates, a system with N_u attached motors has a constant total attachment rate of $\sum_{i:Q^{(i)}=0} a^{(i)}$. Under constant detachment rates $d^{(i)}$, $i = 1, \ldots, N$, which occur when $\Upsilon^{(i)}$ is a constant function, switching between states is a homogeneous, continuous time, finite state Markov chain, with an average time $\tau(\mathbf{S})$ spent in a state $\mathbf{Q} = (Q^{(1)}, \ldots, Q^{(N)})$ given by:

$$\tau(\mathbf{S}) = \frac{1}{\sum_{j=1}^{N} (1 - Q^{(j)}) a^{(j)} + \sum_{j=1}^{N} Q^{(j)} d^{(j)}}. \tag{9}$$

For more complicated detachment rates, the average time until either first detachment or attachment admits no explicit solutions. As we will see in Section 4, however, under a slow switching regime, we may approximate detachment rates by constants $\bar{d}^{(i)}$ through averaging over possible motor-cargo configurations. This is in contrast to the quasi-steady state model studied by Bressloff and Newby [72], in which transitions between states are considered fast compared to motor velocities.

3 Nondimensionalization and averaging

In this section, we prepare for the asymptotic analysis to coarse-grain the detailed model from Section 2 by a systematic nondimensionalization in Subsection 3.1. We thereby identify the detached motor and cargo dynamics as faster than those of the attached motors, and conduct in Subsection 3.2 a stochastic averaging over the cargo and detached motor coordinates to obtain an effective description only involving the attachment state of the

motors together with the spatial positions of attached motors. This section is essentially a generalization of the analysis from McKinley, Athreya, et al [34] to the case of nonidentical cooperative motors, together with a consideration of the coarse-grained attachment or detachment events.

3.1 Nondimensionalization

For the purposes of reducing the number of parameters in a motor-cargo system, we perform a nondimensionalization of (1)-(4), adapting the nondimensionalizaton in [34] for the case of identical cooperative motors. To not only nondimensionalize but normalize the variables for the asymptotic reduction exploiting time scale disparities [73, 74], a reference time scale of γ/κ and a reference length scale of $\sqrt{2k_BT/\kappa}$ was taken in the nondimensionalization, where κ was the common motor-cargo tether spring constant. These characterize the nominal fluctuation dynamics of the cargo, so the resulting nondimensional equations are normalized to order unity for the cargo, and manifest the relatively slow dynamics of the attached motors.

To extend this nondimensionalization to nonidentical motors, we define

$$\bar{\kappa} = \sum_{j=1}^{N} \kappa^{(j)} / N, \quad \widetilde{\kappa}^{(i)} = \kappa^{(i)} / \bar{\kappa}, \tag{10}$$

and take the average $\bar{\kappa}$ to define the reference units in the nondimensionalization. Under the change of coordinates $\tilde{t} = \bar{\kappa}t/\gamma$, and

$$\widetilde{X}^{(i)}(\tilde{t}) = \frac{X^{(i)}(\gamma\tilde{t}/\bar{\kappa})}{\sqrt{2k_BT/\bar{\kappa}}}, \qquad \widetilde{Z}(\tilde{t}) = \frac{Z(\gamma\tilde{t}/\bar{\kappa})}{\sqrt{2k_BT/\bar{\kappa}}}, \tag{11}$$

equations (1) and (2) may be written in nondimensional form

$$\begin{aligned} d\widetilde{X}^{(i)}(\tilde{t}) &= \left(\varepsilon^{(i)} g(s^{(i)}(\widetilde{X}^{(i)}(\tilde{t}) - \widetilde{Z}(\tilde{t})))d\tilde{t} + \sqrt{\widehat{\rho}^{(i)}\varepsilon^{(i)}}dW^{(i)}(\tilde{t})\right)Q^{(i)}(\tilde{t}) \\ &+ \left(-(\Gamma^{(i)})^{-1}\widetilde{\kappa}^{(i)}(\widetilde{X}^{(i)}(\tilde{t}) - \widetilde{Z}(\tilde{t}))d\tilde{t} + (\Gamma^{(i)})^{-1/2}dW^{(i)}(\tilde{t})\right)(1 - Q^{(i)}(\tilde{t})), \\ &1 \le i \le N, \end{aligned} \tag{12}$$

$$d\widetilde{Z}(\tilde{t}) = \left(\sum_{j=1}^{N} \widetilde{\kappa}^{(j)}(X^{(j)}(\tilde{t}) - \widetilde{Z}(\tilde{t})) - \widetilde{F}_T\right)d\tilde{t} + dW_z(\tilde{t}). \tag{13}$$

The nondimensional attachment and detachment rates are now $\tilde{a}^{(i)} = a^{(i)}\gamma/\bar{\kappa}$ and $\tilde{d}^{(i)} = d^{(i)}\gamma/\bar{\kappa}$. Under this nondimensionalization, the detachment rate (5) then becomes (expressed now as a stochastic process in time):

$$\tilde{d}^{(i)}(\tilde{t}) = \tilde{d}_0^{(i)} Y(u^{(i)}(\widetilde{X}^{(i)}(\tilde{t}) - \widetilde{Z}(\tilde{t}))). \tag{14}$$

A listing of nondimensional parameters introduced in Eqs. (12)-(14) and their typical values are provided in Table 2.

3.2 Multiscale Averaging

By comparing magnitudes of drift coefficients, we are now able to identify fast and slow variables. For systems with multiple scales, a common method of dimension reduction averages out fast variables by considering their stationary distributions against fixed values of slow variables (see Pavliotis and Stuart [75] for multiple examples). We will use standard asymptotic notation for indicating the relative magnitudes of quantities. Informally, $f \ll g$ or equivalently $f \sim o(g)$ means f is much smaller than g, $f \sim g$ or equivalently $f \sim ord(g)$ means f and g are of comparable size, $f \gg g$ means f is much greater than g, and $f \sim O(g)$ means f is comparable to or smaller than g. All these concepts can be given precise asymptotic definitions [76], which we follow though without making the formalism explicit. From Table 2 and Eqs. (12) and (13), we observe that a plausible asymptotic ordering for the nondimensional parameters is: $\tilde{a}^{(i)} \sim \tilde{d}^{(i)} \ll \varepsilon^{(i)} \ll 1 \ll (\Gamma^{(i)})^{-1}$. That is, the dynamics for detached motors are faster than those for the cargo, which in turn are faster than those for attached motors, which in turn are faster than the attachment and detachment processes. We by no means claim this asymptotic ordering is well satisfied for all molecular motors, or for kinesin-1 under all conditions, but simply that the assumptions on which our asymptotic simplification is based is at least plausible based on the kinesin-1 data we have drawn from the literature, summarized in nondimensional form in Table 2. The assumption that the attachment and detachment processes are asymptotically slow compared to attached motor dynamics was also adopted and exploited in Miles, Lawley, and Keener [31]. For mixtures of motors, while we allow the attachment, detachment, and unencumbered velocities to differ, we assume the parameters in each group are of the same order of magnitude in our asymptotic ordering ($\tilde{a}^{(i)} \sim \tilde{a}^{(i')} \sim \tilde{d}^{(i)} \sim \tilde{d}^{(i')}$, $\varepsilon^{(i)} \sim \varepsilon^{(i')}$ for all $1 \le i, i' \le N$).

While the focus for this paper will mainly be for two motor systems, it is possible to write averaged formulas for both detached motor and cargo positions under a generic system of N motors. Fixing a time $t \ge 0$ and motor index i, if $Q^{(i)}(t) = 0$, we may regard the distribution of the detached motor $\tilde{X}^{(i)}(t)$ as approximately that of the quasistationary distribution $p_{\tilde{X}^{(i)} \mid \tilde{Z}}$ under fast detached phase dynamics ($Q^{(i)}(t) = 0$ in Eq. 12), with the slower cargo variable $\tilde{Z}(\tilde{t})$ held at a fixed value $\tilde{z}$. This is the Gaussian PDF

$$p_{\tilde{X}^{(i)} \mid \tilde{Z}}(\tilde{x} \mid \tilde{z}) = \sqrt{\frac{\tilde{\boldsymbol{\kappa}}^{(i)}}{\pi}} \exp\left(-\tilde{\boldsymbol{\kappa}}^{(i)}(\tilde{x} - \tilde{z})^2\right), \tag{15}$$

and all detached motor positions are conditionally independent given the cargo position $\tilde{Z}(\tilde{t}) = \tilde{z}$. Similarly, by fixing the positions of the slow attached motors, an approximation of the distribution of the faster cargo position is the quasi-stationary distribution $p_{\tilde{Z} \mid \tilde{\mathbf{X}}^{(a)}}$ of (13) with the states of all motors and the positions of the attached motors held at fixed values, which is another Gaussian of the form

$$p_{\widetilde{Z}\mid\widetilde{\mathbf{X}}^{(a)},\mathbf{Q}}(\widetilde{z}\mid\mathbf{x},\mathbf{q}) = \sqrt{\frac{\sum_{j=1}^{N} q^{(j)}\widetilde{\boldsymbol{\kappa}}^{(j)}}{\pi}}\exp\left[-\left(\sum_{j=1}^{N} q^{(j)}\widetilde{\boldsymbol{\kappa}}^{(j)}\right)\left(\widetilde{z}-\left[\frac{\sum_{i=1}^{N} q^{(j)}\widetilde{\boldsymbol{\kappa}}^{(j)}\widetilde{x}^{(j)}-\widetilde{F}_T}{\sum_{i=1}^{N} q^{(j)}\widetilde{\boldsymbol{\kappa}}^{(j)}}\right]\right)^2\right], \tag{16}$$

where $\mathbf{x} = (x^{(1)}, x^{(2)}, \ldots, x^{(N)})$ and $\mathbf{q} = (q^{(1)}, q^{(2)}, \ldots, q^{(N)})$ parameterize, respectively the positions and states of all N motors. Note that the above formula for the quasistationary distribution of the cargo does not actually depend on the positions of the detached motors (indices i for which $q^{(i)} = 0$), as these are fast relative to the cargo, and so are treated as already averaged out on the cargo time scale. This is why we denote the fixed variable as $\widetilde{\mathbf{X}}^{(a)}$, though we write the quasi-stationary distribution formally as a function of all motor positions to keep notation simple. Moreover, the averaging of the detached motors does not affect the cargo dynamics to leading order, because the tether force will average to zero, and the contribution of the force fluctuations to the cargo diffusivity are $O(\Gamma^{(i)})$. The average position for the cargo according to Eq. (16) is a weighted average of the attached motor positions shifted by a multiple (which would be the simple inverse of the number of attached motors if they had the same tether spring constants) of the nondimensional trap force. In reality the cargo should lag a bit from this weighted average position of the attached motors because of balancing the viscous drag force. Our treatment of $\varepsilon^{(i)}$ as a small parameter, however, implies that the cargo drag force is being treated as small compared to the force scale of the thermal fluctuations of the cargo, so this mean lag would be small compared to the standard deviation of the cargo fluctuations and is thus neglected. We will often refer to (16) in the specific case of systems with $N = 2$ motors. With one out of the two motors attached,

$$\begin{aligned} p_{\widetilde{Z}\mid\widetilde{\mathbf{X}}^{(a)},\mathbf{Q}}(\widetilde{z}\mid(\widetilde{x}^{(1)},\widetilde{x}^{(2)}),(1,0)) &= \sqrt{\frac{\widetilde{\boldsymbol{\kappa}}^{(1)}}{\pi}}\exp\left[-\widetilde{\boldsymbol{\kappa}}^{(1)}\left(\widetilde{z}-\widetilde{x}^{(1)}+\frac{\widetilde{F}_T}{\widetilde{\boldsymbol{\kappa}}^{(1)}}\right)^2\right], \\ p_{\widetilde{Z}\mid\widetilde{\mathbf{X}}^{(a)},\mathbf{Q}}(\widetilde{z}\mid(\widetilde{x}^{(1)},\widetilde{x}^{(2)}),(0,1)) &= \sqrt{\frac{\widetilde{\boldsymbol{\kappa}}^{(2)}}{\pi}}\exp\left[-\widetilde{\boldsymbol{\kappa}}^{(2)}\left(\widetilde{z}-\widetilde{x}^{(2)}+\frac{\widetilde{F}_T}{\widetilde{\boldsymbol{\kappa}}^{(2)}}\right)^2\right], \end{aligned} \tag{17}$$

and with both motors attached,

$$p_{\widetilde{Z}\mid\widetilde{\mathbf{X}}^{(a)},\mathbf{Q}}(\widetilde{z}\mid(\widetilde{x}^{(1)},\widetilde{x}^{(2)}),(1,1)) = \sqrt{\frac{2}{\pi}}\exp\left[-2\left(\widetilde{z}-\frac{\widetilde{\boldsymbol{\kappa}}^{(1)}\widetilde{x}^{(1)}+\widetilde{\boldsymbol{\kappa}}^{(2)}\widetilde{x}^{(2)}}{2}+\frac{\widetilde{F}_T}{2}\right)^2\right]. \tag{18}$$

Our nondimensionalization set the time scale to be order unity for the cargo, so the dynamics of the slower attached motors expressed in Eq. (12) appears weak on this time scale ($ord(\varepsilon^{(i)})$ drift and diffusivity for attached motors i, with $\varepsilon^{(i)} \ll 1$). Thus, to see nontrivial attached motor dynamics, we must go to a longer time scale

$$\widetilde{t} = \bar{t}\,/\,\bar{\varepsilon}, \quad \bar{\varepsilon} = \sum_{j=1}^{N} \varepsilon^{(j)}\,/\,N, \tag{19}$$

over which the cargo now appears $ord((\bar{\varepsilon})^{-1})$ fast and equilibrates quickly relative to changes in attached motor position. From stochastic averaging theory (see [77, 78]), we can approximate the attached motor positions on this time scale $\tilde{X}^{(i)}(\bar{t}\,/\,\bar{\varepsilon})$ by an averaged stochastic process $\bar{X}^{(i)}(\bar{t})$ satisfying the system of SDEs

$$d\bar{X}^{(i)}(\bar{t}) = \bar{g}^{(i)}(\{\bar{X}^{(i)}\}_{i=1}^{N}(\bar{t}); \{Q^{(i)}\}_{i=1}^{N})d\bar{t} + \sqrt{\boldsymbol{\rho}^{(i)}}dW^{(i)}(\bar{t}), \qquad \boldsymbol{\rho}^{(i)} = \frac{\boldsymbol{\varepsilon}^{(i)}}{\bar{\varepsilon}}\hat{\boldsymbol{\rho}}^{(i)}, \tag{20}$$

with an effective drift obtained by averaging over the quasi-stationary distribution of the cargo:

$$\bar{g}^{(i)}(\mathbf{x};\mathbf{s}) = \frac{\boldsymbol{\varepsilon}^{(i)}}{\bar{\varepsilon}}\int_{\mathbb{R}} g(s^{(i)}(\tilde{x}^{(i)} - \tilde{z}))p_{\tilde{Z}\,|\,\tilde{\mathbf{X}}^{(a)},\mathbf{Q}}(\tilde{z}\,|\,\mathbf{x},\mathbf{q})d\tilde{z}\,. \tag{21}$$

Note the averaged dynamics of the attached motors in Eq. (20) are coupled directly to each other, through the averaging out of the cargo variable to which they are explicitly coupled in (12). The averaged drift $\bar{g}^{(i)}$ ostensibly depends on all motor positions, but it actually is independent of the detached motor positions because the same is true of $p_{\tilde{Z}\,|\,\tilde{\mathbf{X}}^{(a)},\mathbf{Q}}$ in Eq. (16). Bouzat [26] proposes alternatively to coarse-grain the effects of the cargo fluctuations on the effective velocity of motors through an exponential time-averaging of the force felt from the cargo. This should give equivalent results to the more straightforward stochastic averaging used here for the "robust" regime of averaging time scales advocated in [26].

Continuing with our assumption that the detachment process is slow compared to the time scale of motor motion ($\tilde{d}^{(i)} \ll \boldsymbol{\varepsilon}^{(i)}$), we may also obtain an averaged detachment rate $\bar{d}^{(i)}(\mathbf{x})$ for each motor i (within the framework [79] of averaging for general Markov processes):

$$\bar{d}^{(i)}(\mathbf{x},\mathbf{s}) = \frac{\tilde{d}_0^{(i)}}{\bar{\varepsilon}}\int_{\mathbb{R}} Y\left(u^{(i)}\left(\tilde{x}^{(i)} - \tilde{z}\right)\right)p_{\tilde{Z}\,|\,\tilde{\mathbf{X}}^{(a)},\mathbf{Q}}(\tilde{z}\,|\,\mathbf{x},\mathbf{q})d\tilde{z}\,. \tag{22}$$

This formula may be viewed as a more detailed implementation of the idea given in [60, 56] that the effective detachment rate for a motor should be computed by averaging the nominal force-detachment rate formula over a probability distribution of forces felt from the cargo, and that this can lead to a significant enhancement relative to the evaluation of the detachment rate in terms of simply the average force felt from the cargo. The constant attachment rates on the longer time scale (19) are now

$$\bar{a}^{(i)} = \tilde{a}^{(i)}\,/\,\bar{\varepsilon}\,. \tag{23}$$

When a detached motor attaches, its attachment position is taken to be drawn from the quasi-stationary distribution of the detached motors, given fixed positions of the attached motors. This follows from our modeling of the attachment process as independent of spatial configuration in the present work. [32, 26, 67] place attaching motors uniformly at random

over the region of the microtubule where the motor-cargo tether is unstretched; this would be roughly consistent with our approach when the linear spring is modified to give no resistance to compression below a rest length (see Appendix A). [55] places attaching motors at the closest position on the microtubule to their attachment point to the cargo (which, with our point particle representation of the cargo, would here amount to attaching the motor at the current cargo position $\widetilde{Z}$). Because of the assumed time scale separation, the relative position of the detached motors and the cargo is independent of the relative position of the cargo and the attached motors, and these are governed by the respective Gaussian quasi-stationary distributions (15) and (17). The quasi-stationary distribution of the position of the detached motors for fixed positions of the attached motors is therefore obtained by convolving these Gaussian quasi-stationary distributions, giving rise to a Gaussian distribution as well. In the simple case of $N = 2$ motors with exactly one of the two motors currently attached, the probability densities for the attachment position of the detached motor would be:

$$p^{(a)}_{\widetilde{X}^{(2)}}(x' \mid (\widetilde{x}^{(1)}, \widetilde{x}^{(2)}), (1,0)) = \int_{\mathbb{R}} p_{\widetilde{X}^{(i)} \mid \widetilde{Z}}(x' \mid \widetilde{z}) p_{\widetilde{Z} \mid \widetilde{\mathbf{X}}^{(a)}, \mathbf{Q}}(\widetilde{z} \mid (\widetilde{x}^{(1)}, \widetilde{x}^{(2)}), (1,0)) d\widetilde{z} = \sqrt{\frac{\widetilde{\boldsymbol{\kappa}}^{(1)}\widetilde{\boldsymbol{\kappa}}^{(2)}}{2\pi}} \exp\left(-\frac{\widetilde{\boldsymbol{\kappa}}^{(1)}\widetilde{\boldsymbol{\kappa}}^{(2)}}{2}\left(x' - \widetilde{x}^{(1)} + \frac{\widetilde{F}}{\widetilde{\boldsymbol{\kappa}}^{(1)}}\right)^2\right), \tag{24}$$

$$p^{(a)}_{\widetilde{X}^{(1)}}(x' \mid (\widetilde{x}^{(1)}, \widetilde{x}^{(2)}), (0,1)) = \sqrt{\frac{\widetilde{\boldsymbol{\kappa}}^{(1)}\widetilde{\boldsymbol{\kappa}}^{(2)}}{2\pi}} \exp\left(-\frac{\widetilde{\boldsymbol{\kappa}}^{(1)}\widetilde{\boldsymbol{\kappa}}^{(2)}}{2}\left(x' - \widetilde{x}^{(2)} + \frac{\widetilde{F}}{\widetilde{\boldsymbol{\kappa}}^{(2)}}\right)^2\right). \tag{25}$$

For the general case of N motors, the attachment position of a currently detached motor i would have a Gaussian probability distribution with mean

$$\frac{\sum_{j=1}^{N} q^{(j)} \widetilde{\boldsymbol{\kappa}}^{(j)} \widetilde{x}^{(j)} - \widetilde{F}_T}{\sum_{j=1}^{N} q^{(j)} \widetilde{\boldsymbol{\kappa}}^{(j)}}$$

and variance

$$\frac{1}{2\sum_{j=1}^{N} q^{(j)} \widetilde{\boldsymbol{\kappa}}^{(j)}} + \frac{1}{2\widetilde{\boldsymbol{\kappa}}^{(i)}}.$$

4 Effective dynamics under slow switching approximation

From here on, we will focus on dynamics for a two motor ($N = 2$) system during a processive run. At any one time, either one or two motors may be attached to the microtubule, which gives three possible states, or the run may terminate when both motors are simultaneously detached from the microtubule. The dynamical description for $N = 2$ motors resulting from the coarse-graining over the dynamics of detached motors and cargo fluctuations is summarized in Figure 2. The cargo position is now represented as a probability distribution given the location and identity of the attached motors (see Eq. (28)),

with a "cargo tracking variable" $M(\bar{t})$ representing the conditional mean position of the cargo. The symmetry of the dynamics under common spatial translation of all entities implies the effective dynamics while in the state with one motor attached has constant drift and attachment/detachment rates, while these quantities in the state with two motors attached only depends on the directed separation of the attached motors

$$R(\bar{t}) \equiv \bar{X}^{(1)}(\bar{t}) - \bar{X}^{(2)}(\bar{t}) . \tag{26}$$

In this section, we will make use of the assumption that the attachment and detachment rates are slow relative to the attached motor dynamics ($\tilde{a}, \tilde{d} \ll \varepsilon$), to homogenize the spatial dynamics within each attachment state and thereby further coarse-grain our model, based on stochastic differential equations with configuration-dependent detachment rates, into simple continuous-time Markov chain dynamics on the state space of attachment states, together with the cargo tracking variable $M(t)$ which may be thought of as an accumulated reward function associated with the Markov chain. The four states of this Markov chain are labeled by a list $\bar{\boldsymbol{\omega}}$ of the indices of the attached motors, as indicated in Figure 3. The transition rates between states after homogenization of attached motor dynamics are now all constant, also indicated in Figure 3.

The state $\bar{\boldsymbol{\omega}} = \varnothing$ acts as an absorbing state terminating the processive run. In each the other three states, the cargo tracking variable undergoes a constant-coefficient drift-diffusion dynamics. Thus, a visit to a state $\bar{\boldsymbol{\omega}} \neq \varnothing$ is associated to a cargo tracking variable increment

$$\Delta M_{\bar{\omega}} = V_{\bar{\omega}} \Delta T_{\bar{\omega}} + \sqrt{2 D_{\bar{\omega}}} \Delta W(\Delta T_{\bar{\omega}}),$$

where $\Delta T_{\bar{\boldsymbol{\omega}}}$ is the duration of the visit to state $\bar{\boldsymbol{\omega}}$, $V_{\bar{\boldsymbol{\omega}}}$ and $D_{\bar{\boldsymbol{\omega}}}$ are, respectively, the constant coarse-grained velocity and diffusivity in state $\bar{\boldsymbol{\omega}}$, and $\Delta W(t) \sim N(0, t)$ denotes the increment of the Wiener process over a time t. In other words, the cargo tracking variable increment is Gaussian conditioned on the duration $\Delta T_{\bar{\boldsymbol{\omega}}}$ in the state $\bar{\boldsymbol{\omega}}$:

$$\Delta M_{\bar{\omega}} \mid \Delta T_{\bar{\omega}} \sim N(V_{\bar{\omega}} \Delta T_{\bar{\omega}}, 2 D_{\bar{\omega}} \Delta T_{\bar{\omega}}) . \tag{27}$$

Here and later, the notation $Y \sim N(\mu, \sigma^2)$ indicates that Y is a normally distributed random variable with mean μ and variance σ^2. The tracking variable M will also suffer jumps associated to transitions, corresponding to adjustments in the mean cargo position under the new configuration of attached motors.

We now proceed to more precisely quantify the elements of the coarse-grained Markov chain description depicted in Figure 3. The cargo tracking variable M for the motor-cargo complex in the coarse-grained representation is defined and discussed in Subsection 4.1. Thereafter, formulas for the effective drift and diffusion coefficients of the cargo tracking variable in each state ($V_{\bar{\boldsymbol{\omega}}}$ and $D_{\bar{\boldsymbol{\omega}}}$) are presented in Subsection 4.2. In Subsection 4.3, we describe both the transition rates of the coarse-grained Markov chain as well as the associated jumps in the tracking variable at a transition. These coarse-grained quantities are

expressed following the nondimensionalization from Subsection 3.1, followed by the passage to the long time scale $\bar{t} = \tilde{t}\bar{\varepsilon}$, so the effective drift, diffusion, and attachment/detachment rate formulas presented would need to be multiplied by $\bar{\varepsilon}$ to give their expressions in terms of the original nondimensionalization. Note that when describing effective transport and switching rates from various states of attachment, we will typically list the indices of the attached motors in the subscript (without parentheses or brackets), and when needed, indicating by a parenthesized superscript the index of which motor in that state is being described by the parameter. Finally, in Subsection 4.4, we shift focus to a more event-based view, decomposing the progress of a motor-cargo complex along a microtubule in terms of cycles of detachment and reattachment of a motor before eventual complete detachment of both motors. This representation of the motor-cargo complex dynamics in terms of these cycles will be the basis for computing the overall statistics of cargo transport in Section 5.

4.1 Tracking Variable for Coarse-Grained Motor-Cargo Complex

One challenge in characterizing the progress of the motor-cargo system through phases of attachment and detachment is the choice of a "tracking" variable that remains well-defined in the various states of motor attachment. The cargo variable $\widetilde{Z}(\tilde{t})$ is an obvious candidate since in experiments it is the largest and most easily observed object, and whose progress through space is of practical importance. Mathematically, though, as shown in the dimensional analysis from Subsection 3.1, the cargo will tend to fluctuate more rapidly than attached motors, which makes it somewhat awkward to use its instantaneous position as a tracking variable on long time scales. We therefore introduce the variable $\widetilde{M}(\tilde{t})$ for the mean cargo position at time $\tilde{t}$ under the quasi-stationary distribution $p_{\widetilde{Z} \mid \widetilde{\mathbf{X}}^{(a)}, \mathbf{Q}}$ (16) for the cargo given the current positions of the motors attached to the microtubule at time $\tilde{t}$:

$$\begin{aligned} \widetilde{M}(\tilde{t}) &\equiv \int_{-\infty}^{\infty} \tilde{z}\, p_{\widetilde{Z} \mid \widetilde{\mathbf{X}}^{(a)}, \mathbf{S}}(\tilde{z} \mid \widetilde{\mathbf{X}}(\tilde{t}), \mathbf{Q}(\tilde{t})) \\ &= \left[\frac{\sum_{j=1}^{N} Q^{(j)}(\tilde{t}) \tilde{\kappa}^{(j)} \widetilde{X}^{(j)}(\tilde{t})}{\sum_{j=1}^{N} Q^{(j)}(\tilde{t}) \tilde{\kappa}^{(j)}} - \frac{\widetilde{F}_T}{\sum_{j=1}^{N} Q^{(j)}(\tilde{t}) \tilde{\kappa}^{(j)}} \right]. \end{aligned} \tag{28}$$

One can check that $\widetilde{M}(\tilde{t})$ is equivalent to the deterministic mechanical equilibrium of the cargo, for given attached motor positions, in the absence of stochastic fluctuations. Markov chain models for cargo transport with attaching and detaching motors often model the cargo as always being exactly at this position $\widetilde{M}(\tilde{t})$ of force balance relative to the attached motors [13, 24]; our present model accounts for cargo fluctuations about this mechanical equilibrium. Nonetheless, $\widetilde{M}$ is a more convenient variable for tracking the progress of the cargo through episodes of attachment and detachment. Moreover, the cargo position $\widetilde{Z}(\tilde{t})$, under our time scale separation assumptions, has a Gaussian distribution centered at $\widetilde{M}(\tilde{t})$ with standard deviation no larger than $\max_{1 \le j \le N}\{\frac{1}{2\tilde{\kappa}^{(j)}}\}$ (see Eq. (16)). Consequently, the long-time statistical transport properties of the cargo position $\widetilde{Z}(\tilde{t})$ and the tracking variable

$\widetilde{M}(\tilde{t})$ are equivalent. Note below we define the tracking variable on the longer time scale (which is being used after averaging out the cargo dynamics in Subsection 3.2) as

$$M(\bar{t}) = \widetilde{M}(\bar{t} \,/\, \bar{\varepsilon})\,. \tag{29}$$

4.2 Effective Drift and Diffusion Coefficients in Attachment States

For states where the motor with index i is attached but the other motor is detached, the effective drift is:

$$V_i = \sqrt{\frac{\widetilde{\boldsymbol{\kappa}}^{(i)}}{\pi}}\frac{\boldsymbol{\varepsilon}^{(i)}}{\bar{\varepsilon}}\int_{\mathbb{R}} g(s^{(i)}y)\exp(-\widetilde{\boldsymbol{\kappa}}^{(i)}(y - \widetilde{F}_T \,/\, \widetilde{\boldsymbol{\kappa}}^{(i)})^2)dy\,. \tag{30}$$

and the effective diffusivity is

$$D_i = \frac{1}{2}\boldsymbol{\rho}^{(i)}\,. \tag{31}$$

These formulas follow directly from Eq. (20), once we recognize from Eq. (28), that

$$\widetilde{M}(\tilde{t}) = \widetilde{X}^{(i)}(\tilde{t}) - \widetilde{F} \,/\, \widetilde{\boldsymbol{\kappa}}^{(i)}\,. \tag{32}$$

Now we just carry over the result from Eq. (20), noting the expression (21) is constant for the case of one attached motor.

For the state where both motors are attached, the effective drift is:

$$V_{1,2} = \int_{\mathbb{R}} G_+(r)p_R(r)dr\,. \tag{33}$$

Where

$$p_R(r) = C_R\exp\left[\frac{2}{\boldsymbol{\rho}^{(1)} + \boldsymbol{\rho}^{(2)}}\int_0^r G_-(r')dr'\right],\quad -\infty < r < \infty, \tag{34}$$

with normalizing constant C_R, is the stationary probability density for the displacement $R = X^{(1)} - X^{(2)}$ between the two attached motors. The effective diffusivity of the motor-cargo complex in this state is:

$$D_{1,2} = \int_{-\infty}^{\infty}\left(\frac{1}{\boldsymbol{\rho}^{(1)} + \boldsymbol{\rho}^{(2)}}\right)\left(\int_{-\infty}^{r}(G_+(r') - V_{1,2})p_R(r')dr'\right)^2\frac{1}{p_R(r)}dr$$
$$+\left(\frac{\boldsymbol{\rho}^{(1)}\widetilde{\boldsymbol{\kappa}}^{(1)} - \boldsymbol{\rho}^{(2)}\widetilde{\boldsymbol{\kappa}}^{(2)}}{\boldsymbol{\rho}^{(1)} + \boldsymbol{\rho}^{(2)}}\right)\int_{\mathbb{R}}(G_+(r) - V_{1,2})p_R(r)\cdot r dr + \frac{\boldsymbol{\rho}^{(1)}(\widetilde{\boldsymbol{\kappa}}^{(1)})^2 + \boldsymbol{\rho}^{(2)}(\widetilde{\boldsymbol{\kappa}}^{(2)})^2}{8}\,.$$

The auxiliary functions referenced in these formulas are:

$$G_+(r) = \frac{\widetilde{\boldsymbol{\kappa}}^{(1)}}{2} G^{(1)}(r) + \frac{\widetilde{\boldsymbol{\kappa}}^{(2)}}{2} G^{(2)}(r), \tag{35}$$

$$G_-(r) = G^{(1)}(r) - G^{(2)}(r)\,. \tag{36}$$

The derivation of these formulas for the effective transport for the state with two motors attached proceeds as follows. For known motor positions $x^{(1)}$, $x^{(2)}$, we can express the cargo-averaged drift coefficients purely in terms of the signed displacement $r = x^{(1)} - x^{(2)}$ between the motors:

$$\bar{g}^{(1)}(x^{(1)}, x^{(2)}; (1,1)) = G^{(1)}(x^{(1)} - x^{(2)}), \tag{37}$$

$$\bar{g}^{(2)}(x^{(1)}, x^{(2)}; (1,1)) = G^{(2)}(x^{(1)} - x^{(2)}), \tag{38}$$

$$G^{(i)}(r) = \frac{\boldsymbol{\varepsilon}^{(i)}}{\bar{\boldsymbol{\varepsilon}}} \sqrt{\frac{2}{\pi}} \int_{\mathbb{R}} g(s^{(i)} y) \exp\left(-2 \left(y + \frac{(-1)^i \widetilde{\boldsymbol{\kappa}}^{(i')} r}{2} - \frac{\widetilde{F}_T}{2} \right)^2 \right) dy\,. \tag{39}$$

This representation is achieved by the change of variable $y = x^{(i)} - z$ in (21).

The tracking variable (28) in this state is, from Eq. (18),

$$\widetilde{M}(\tilde{t}) = (\widetilde{\boldsymbol{\kappa}}^{(1)} \widetilde{X}^{(1)}(\tilde{t}) + \widetilde{\boldsymbol{\kappa}}^{(2)} \widetilde{X}^{(2)}(\tilde{t}) - \widetilde{F}_T) \,/\, 2, \tag{40}$$

Passing now to the long time scale $\bar{t} \,/\, \boldsymbol{\varepsilon}$, we can recast the cargo-averaged dynamics (20) for the two attached motors in terms of this tracking variable rescaled to large time, $M(\bar{t})$ (29), and the (signed) intermotor separation

$$R(\bar{t}) \equiv \widetilde{X}^{(1)}(\bar{t} \,/\, \bar{\boldsymbol{\varepsilon}}) - \widetilde{X}^{(2)}(\bar{t} \,/\, \bar{\boldsymbol{\varepsilon}})$$

which gives

$$dM(\bar{t}) = G_+(R(\bar{t}))d\bar{t} + \frac{\sqrt{\boldsymbol{\rho}^{(1)}(\widetilde{\boldsymbol{\kappa}}^{(1)})^2}}{2} dW^{(1)}(\bar{t}) + \frac{\sqrt{\boldsymbol{\rho}^{(2)}(\widetilde{\boldsymbol{\kappa}}^{(2)})^2}}{2} dW^{(2)}(\bar{t}), \tag{41}$$

$$dR(\bar{t}) = G_-(R(\bar{t}))dt + \sqrt{\boldsymbol{\rho}^{(1)}} dW^{(1)}(\bar{t}) - \sqrt{\boldsymbol{\rho}^{(2)}} dW^{(2)}(\bar{t})\,. \tag{42}$$

Under the regime where switching is slow relative to detachment, we may simply homogenize the internal variable R in order to obtain the effective velocity and diffusion for M on the long time scales when attachment or detachment occurs. As (42) does not depend

on M, the stationary distribution for the process R is a potential function, given in Eq. (34). The formula (33) follows directly.

The computation for effective diffusivity is more complicated. For nonidentical motors, the driving terms in the stochastic differential equations in Eqs. (41)-(42) are correlated in general, unlike the identical motor case from [34]. Only minor modifications are needed to generalize the derivation for effective diffusion found in Pavliotis and Stuart [75] for the case of uncorrelated stochastic driving, as we show in Appendix B.

4.3 Effective switching dynamics

After presenting in Subsection 4.3.1 the effective switching rates between attachment states (as indicated in Figure 3), we discuss the effectively instantaneous jumps in the cargo tracking variable that occurs in the coarse-grained representation when switches occur. Namely, when a motor i detaches from the two-motor-attached state (transition (1, 2) $\rightarrow$ (i ́)), the tracking variable undergoes a jump $\Delta M_i^{(\mathrm{d})}$ given by equation (52). When a motor i attaches to form the two-motor-attached state (transition (i ́) $\rightarrow$ (1, 2)), the tracking variable undergoes a jump $\Delta M_i^{(\mathrm{a})}$, given by equation (56).

4.3.1 Effective detachment rates—From our assumptions about the detachment time scale being slower than the attached motor time scale ($\tilde{d}^{(i)} \ll \boldsymbol{\varepsilon}^{(i)}$) in Subsection 3.2, we can apply stochastic averaging [79] to approximate the rate at which motor i detaches from a state with both motors attached by averaging over the stationary distribution $p_R(r)$ (34) for the motor separation R, just as we did for the effective velocity:

$$\bar{d}_{1,2}^{*\,(i)} = \int_{\mathbb{R}} \bar{d}_{1,2}^{(i)}(r) p_R(r) dr, \tag{43}$$

$$\bar{d}_{1,2}^{(i)}(r) = \sqrt{\frac{2}{\pi}} \frac{\tilde{d}_0^{(i)}}{\bar{\boldsymbol{\varepsilon}}} \int_{\mathbb{R}} Y\left(u^{(i)} y\right) \exp\left(-2\left(y - \frac{1}{2}((-1)^{i+1} \tilde{\boldsymbol{\kappa}}^{(i')} r - \tilde{F}_T)\right)^2\right) dy\,. \tag{44}$$

This last formula is just an expression of the detachment rate (22) solely through the intermotor distance $r = x^{(1)} - x^{(2)}$, An effective total rate of detachment from the state of both motors attached is then

$$\bar{d}_{1,2}^{*} = \bar{d}_{1,2}^{*\,(1)} + \bar{d}_{1,2}^{*\,(2)}\,. \tag{45}$$

In the case of a single attached motor with index i, we have a constant attachment rate $\tilde{a}^{(i')}$, and detachment rate $\tilde{d}^{(i)}(x^{(i)}, z)$ that is dependent on the attached motor position $x^{(i)}$ and cargo position z. On the longer $\bar{t} = \bar{\boldsymbol{\varepsilon}}\tilde{t}$ time scale, the slow switching approximation would reduce the detachment rate (22) to a constant:

$$\bar{d}_i^* = \sqrt{\frac{\widetilde{\boldsymbol{\kappa}}^{(i)}}{\pi}} \frac{\widetilde{d}_0^{(i)}}{\bar{\boldsymbol{\varepsilon}}} \int_{\mathbb{R}} Y(u^{(i)} y) \exp(-\widetilde{\boldsymbol{\kappa}}^{(i)} (y - \widetilde{F}_T / \widetilde{\boldsymbol{\kappa}}^{(i)})^2) dy \,. \tag{46}$$

and simply rescale the constant attachment rates:

$$\bar{a}^{*(i)} \equiv \frac{\widetilde{a}^i}{\bar{\boldsymbol{\varepsilon}}} \,. \tag{47}$$

4.3.2 Jumps at detachment from state of both motors attached—When a motor detaches from a state of two attached motors, there is an immediate change in the force balance between motors and cargo. The cargo, which is fast relative to a single bound motor, quickly adjusts to the new motor configuration. This results in a jump of the tracking variable position. A similar readjustment occurs with motor attachment. See Fig. 4 in Section 6 for simulations depicting jumps in cargo positions. In this subsection, we describe distributions of jump sizes at these switching events. This is done under the assumption of slow switching, so that we may assume the intermotor distance variable $R(\bar{t})$ in the state of two attached motors (in addition to the cargo) has achieved its stationary distribution.

We focus in this subsection on the statistical behavior of the system at a random time τ_{d} at which one of the two motors detaches ($\mathbf{Q}(\tau_{\mathrm{d}}^-) = (1,1) \neq \mathbf{Q}(\tau_{\mathrm{d}})$). The distribution of $R(\tau_{\mathrm{d}}^-)$ just before detachment will not be the same as the stationary distribution of $R(t)$ due to the dependence of the detachment rate on $R(t)$. Rather, the distribution of the intermotor distance just before first detachment $R^{(\mathrm{d})} = R(\tau_{\mathrm{d}}^-)$ will be reweighted by the detachment rate, yielding the probability density:

$$p_{R^{(\mathrm{d})}}(r) = \frac{(\bar{d}_{1,2}^{(1)}(r) + \bar{d}_{1,2}^{(2)}(r)) p_R(r)}{\bar{d}_{1,2}^*} \,. \tag{48}$$

This can be readily argued by considering a short time interval of length Δt over which fluctuations in $R(t)$ are negligible, using Bayes' rule to calculate the conditional probability of $R(t)$ given that detachment occurs during the time interval, and passing to the limit $\Delta t \downarrow 0$.

Next, we denote by $J^{(d)}$ the index of the motor which first detaches from the two-motor-attached state (at the random time τ_{d}). From the standard theory of continuous-time jump processes,

$$\mathbb{P}(J^{(d)} = i \mid R(\tau_{\mathrm{d}}) = r) = \frac{\bar{d}_{1,2}^{(i)}(r)}{\bar{d}_{1,2}^{(1)}(r) + \bar{d}_{1,2}^{(2)}(r)}, \tag{49}$$

and thus the unconditional probability that motor i detaches first is:

$$p_d^{(i)} \equiv \mathbb{P}(J^{(d)} = i) = \int_{-\infty}^{\infty} \frac{\bar{d}_{1,2}^{(i)}(r)}{\bar{d}_{1,2}^{(1)}(r) + \bar{d}_{1,2}^{(2)}(r)} p_{R^{(\mathrm{d})}}(r)dr = \frac{\bar{d}_{1,2}^{*(i)}}{\bar{d}_{1,2}^{*}}. \tag{50}$$

This is consistent with the coarse-grained description of the attachment states of the motors, under the slow switching approximation, having the properties of a continuous-time Markov chain.

The jump of the tracking variable M at detachment is essentially a result of how the mean position of cargo relies upon the number of attached motors. This is represented by the difference between equations (32) and (40). Consider, for now, that motor 2 detaches ($J^{(d)} = 2$) from the two-motor-attached state at time τ_{d}. The jump size $\Delta M_2^{(\mathrm{d})} = M(\tau_{\mathrm{d}}) - M(\tau_{\mathrm{d}}^-)$ will be

$$\begin{aligned}\Delta M_2^{(\mathrm{d})} &= \left[\bar{X}^{(1)}(\tau_{\mathrm{d}}^-) - \frac{\widetilde{F}}{\widetilde{\boldsymbol{\kappa}}^{(1)}}\right] - \frac{1}{2}\left[\widetilde{\boldsymbol{\kappa}}^{(1)}\bar{X}^{(1)}(\tau_{\mathrm{d}}^-) + \widetilde{\boldsymbol{\kappa}}^{(2)}\bar{X}^{(2)}(\tau_{\mathrm{d}}^-) - \widetilde{F}\right] \\ &= \frac{\widetilde{\boldsymbol{\kappa}}^{(2)}}{2} R(\tau_{\mathrm{d}}^-) - \frac{\widetilde{\boldsymbol{\kappa}}^{(2)}\widetilde{F}}{2\widetilde{\boldsymbol{\kappa}}^{(1)}}.\end{aligned}$$

and thus have the distribution

$$\Delta M_2^{(\mathrm{d})} \sim \frac{\widetilde{\boldsymbol{\kappa}}^{(2)}}{2}\left(R_2^{(d)} - \frac{\widetilde{F}}{\widetilde{\boldsymbol{\kappa}}^{(1)}}\right).$$

where $R_i^{(d)}$ is defined as a random variable with distribution equal to that of the intermotor distance $R^{(\mathrm{d})}$ conditioned on the event $J^{(d)} = i$ that motor i is the one which detaches from the state of both motors attached. Using Bayes' rule with Eqs. (49)-(50), we can derive the probability density function

$$p_{R_i^{(d)}} = \frac{p_R(r)\bar{d}_{1,2}^{(i)}(r)}{\bar{d}_{1,2}^{*(i)}}. \tag{51}$$

A similar calculation shows that when motor 1 detaches ($J^{(d)} = 1$), then $\Delta M_1^{(\mathrm{d})} \sim \frac{\widetilde{\boldsymbol{\kappa}}^{(1)}}{2}(-R_1^{(d)} - \frac{\widetilde{F}}{\widetilde{\boldsymbol{\kappa}}^{(2)}})$. In more compact form, the jump in the tracking variable when motor i detaches first from the two-motor-attached state has distribution:

$$\Delta M_i^{(\mathrm{d})} \sim \frac{\widetilde{\boldsymbol{\kappa}}^{(i)}}{2}\left((-1)^i R_i^{(d)} - \frac{\widetilde{F}}{\widetilde{\boldsymbol{\kappa}}^{(i')}}\right), \tag{52}$$

4.3.3 Jumps at attachment of second motor from state of one motor attached

—We now compute the statistics of the jumping distances at a time τ_{a} before which only one

motor is attached, and at which time the second motor (with index $\mathcal{J}^{(a)}$) attaches. Suppose first that we begin with motor 1 attached, then motor 2 attaches ($\mathcal{J}^{(a)} = 2$) at time τ_a.

From Eq. (24), detached motor 2 has a location distributed, conditional on the position of attached motor 1, as

$$\bar{X}^{(2)}(\tau_a^-) \sim N(\bar{X}^{(1)}(\tau_a^-) - \widetilde{F}_T \,/\, \widetilde{\kappa}^{(1)}, 1 \,/\, (\widetilde{\kappa}^{(1)}\widetilde{\kappa}^{(2)}))\,. \tag{53}$$

Under our model that the attaching motors attaches at a position governed by its detached spatial distribution, the jump in the central coordinate upon attachment of motor 2 is then

$$\begin{aligned} \Delta M_2^{(a)} &= \frac{1}{2}\left[\widetilde{\kappa}^{(1)}\bar{X}^{(1)}(\tau_a^-) + \widetilde{\kappa}^{(2)}\bar{X}^{(2)}(\tau_a^-) - \widetilde{F}_T\right] - \left[\bar{X}^{(1)}(\tau_a^-) - \frac{\widetilde{F}_T}{\widetilde{\kappa}^{(1)}}\right] \\ &\sim N\left(0, \frac{\widetilde{\kappa}^{(2)}}{4\widetilde{\kappa}^{(1)}}\right). \end{aligned} \tag{54}$$

More generally, when motor i is the detached motor which attaches, the tracking coordinate jumps by an amount

$$\Delta M_i^{(a)} \sim N\left(0, \frac{\widetilde{\kappa}^{(i)}}{4\widetilde{\kappa}^{(i')}}\right), \tag{55}$$

which is always mean zero even when the motors are nonidentical. We remark that the reattachment rule of Keller, Berger, et al [25], where the tether between the detached motor and cargo is treated as exactly slack (at rest length), and this motor reattaches similarly at a location where the tether force is zero, and the cargo instantaneously moves to a position of mechanical force balance, corresponds to a deterministic version of the rules described for our model above, using just the means of the random reattachment position and jump in cargo tracking variable.

4.4 Effective dynamics in terms of detachment-attachment cycles

Starting from the fully attached state (1,2), the motor-cargo complex will undergo a random number N_c of *full cycles* between 2-motor and 1-motor attached states (either (1,2) → (1) → (1,2) or (1,2) → (2) → (1,2)) and ultimately a *terminal cycle* (either (1,2) → (1) → 0 or (1,2) → (2) → 0) ending in complete detachment. Thus N_c is a geometric random variable with mean $(1 - p_d^{\varnothing}) \,/\, p_d^{\varnothing}$, where the probability of complete detachment during an initiated cycle is defined by

$$p_d^{\varnothing} = p_d^{(2)}\frac{\bar{d}_1^*}{\bar{a}^{*(2)} + \bar{d}_1^*} + (1 - p_d^{(2)})\frac{\bar{d}_2^*}{\bar{a}^{*(1)} + \bar{d}_2^*}\,. \tag{56}$$

For each cycle (either complete or terminal), time advances by a random increment

$$\Delta T_{\mathrm{c}} = \Delta T_{1,2} + \Delta T_{J^{(d)'}}, \tag{57}$$

where $J^{(d)'} \equiv 3 - J^{(d)}$ is the index of the motor remaining attached.

The distributions of time $\Delta T_{1,2}$ spent in the fully attached and time ΔT_i spent in the state with only motor i attached are exponentially distributed random variables with the indicated means:

$$\Delta T_{1,2} \sim \mathrm{Exp}((\bar{d}^*_{1,2})^{-1}), \quad \Delta T_i \sim \mathrm{Exp}((\bar{a}^{*(i')} + \bar{d}^*_i)^{-1}). \tag{58}$$

Similarly, in each cycle the tracking variable will advance by a random increment

$$\Delta M_{\mathrm{c}} = \Delta M_{1,2} + \Delta M_{J^{(d)'}} + \widetilde{\Delta M}^{(\mathrm{a})}_{J^{(d)}} + \Delta M^{(\mathrm{d})}_{J^{(d)}}. \tag{59}$$

Here, we write $\widetilde{\Delta M}^{(\mathrm{a})}_i$ to extend the random variable $\Delta M^{(\mathrm{a})}_i$ (56) describing the jump in the cargo tracking variable upon reattachment of motor i to omit its contribution (with the value $\widetilde{\Delta M}^{(\mathrm{a})}_i = 0$) in the terminal cycle when motor i' detaches before motor i reattaches. The distributions for the jump in the cargo tracking variable upon detachment of motor i, $\Delta M^{(\mathrm{d})}_i$, is given in Eq. (52). By the independence of residence times and the next state visited in a continuous-time Markov chain, these jumps are independent of the time spent in any state of the cycle. On the other hand, from the results of Subsection 4.2 for the effective velocity and diffusivity in each attachment state,

$$\Delta M_{1,2} \mid \Delta T_{1,2} \sim N(V_{1,2}\Delta T_{1,2}, 2D_{1,2}\Delta T_{1,2}), \tag{60}$$

$$\Delta M_i \mid \Delta T_i \sim N(V_i \Delta T_i, \boldsymbol{\rho}^{(i)} \Delta T_{1,2}). \tag{61}$$

Like the distributions for $\Delta T_{1,2}$ and ΔT_i, the displacements $\Delta M_{1,2}$ and ΔM_i, within an attachment state are independent on whether the motor system eventually returns to a two motor attached state.

5 Effective Transport Characterization

For a cooperative system of two motors, we have provided in the previous section a coarse-grained approximation of the stochastic process governed by equations (12)-(14). These simplified equations are adequate, under the conditions of validity of the asymptotic approximations, for computing effective transport properties of the motor-cargo complex. We begin in Subsection 5.1 by computing the processivity measures: the mean and variance of the run time and run length. Then we turn in Subsection 5.2 to the theoretical calculation of the effective velocity and diffusivity of the motor-cargo complex. The proper definition of these transport statistics is not entirely obvious for a motor-cargo complex that eventually

detaches and terminates progress along the microtubule. We discuss two distinct mathematical framings of velocity and diffusivity in this context, and relate them to approaches used in analyses of previous models as well as to experimental approaches. We then, in turn, compute the velocity and diffusivity under each of the two mathematical interpretations.

The formulas in these subsections are formulated in terms of statistics of the cycles of attachment and detachment presented and derived in Subsection 5.3. In complicated expressions, we will sometimes have μ_Y denote the mean, σ_Y denote the standard deviation, and $\sigma_{Y,Y'}$ denote the covariance of the random variables Y, Y'.

5.1 Run length and run time statistics

We now consider the total run time T and total run length L taken by an ensemble of a cargo with two cooperative motors before complete detachment. For simplicity, we take the system to start with both motors are attached. Then T is just the first passage time of the coarse-grained Markov chain from state (1,2) to the state 0, and L is the increment in the cargo tracking variable M until absorption at the fully detached state 0. We may then write T and L as random sums of iid random variables $\{\Delta T_c^j\}_{j=1}^{\infty}$ and $\{\Delta M_c^j\}_{j=1}^{\infty}$, where the number of complete detachment-attachment cycles N_c (and therefore also the total number of cycles $N_c + 1$) has the property of a Markov (stopping) time for the natural filtration generated by these two sequences of random variables together with the sequence of Markov chain states visited:

$$T = \sum_{j=1}^{N_c+1} \Delta T_c^j, \quad L = \sum_{j=1}^{N_c+1} \Delta M_c^j. \tag{62}$$

This permits us to use Wald's identity (Th. 14.6 of DasGupta [80]) and the second Wald identity (Th. 2.4.5 of Ghosh, Mukhopadhyay, and Sen [81]) to obtain:

Proposition 1 *(Run length and time from cycle statistics)*

1. The mean run time and run length are given by

$$\boldsymbol{\mu}_T \equiv \mathbb{E}[T] = \mathbb{E}[N_c + 1]\boldsymbol{\mu}_{\Delta T_c}, \tag{63}$$

$$\boldsymbol{\mu}_L \equiv \mathbb{E}[L] = \mathbb{E}[N_c + 1]\boldsymbol{\mu}_{\Delta M_c}. \tag{64}$$

2. The variances and covariance of the run time and run length are given by

$$\boldsymbol{\sigma}_T^2 \equiv Var(T) = \mathbb{E}[N_c + 1]\boldsymbol{\sigma}_{\Delta T_c}^2 + Var(N_c + 1)\boldsymbol{\mu}_{\Delta T_c}^2, \tag{65}$$

$$\begin{aligned}\boldsymbol{\sigma}_L^2 &\equiv Var(L) = \mathbb{E}[N_c + 1]\boldsymbol{\sigma}_{\Delta M_c}^2 + Var(N_c + 1)(\boldsymbol{\mu}_{\Delta M_c})^2,\\ \boldsymbol{\sigma}_{T,L} &\equiv Cov(T, L) = \mathbb{E}[N_c + 1]\boldsymbol{\sigma}_{\Delta T_c, \Delta M_c} + Var(N_c + 1)\boldsymbol{\mu}_{\Delta T_c}\boldsymbol{\mu}_{\Delta M_c}.\end{aligned} \tag{66}$$

3. *The number of complete detachment-attachment cycles N_c has the following first and second order statistics:*

$$\mathbb{E}[N_c + 1] = \frac{1}{p_d^{\varnothing}}, \tag{67}$$

$$Var[N_c + 1] = \frac{1 - p_d^{\varnothing}}{p_d^{\varnothing 2}}, \tag{68}$$

with the probability of complete detachment during an initiated cycle given by

$$p_d^{\varnothing} = p_d^{(2)}\frac{\bar{d}_1^*}{\bar{a}^{*(2)} + \bar{d}_1^*} + (1 - p_d^{(2)})\frac{\bar{d}_2^*}{\bar{a}^{*(1)} + \bar{d}_2^*}. \tag{69}$$

The statistics of N_c follow directly from the discussion at the beginning of Subsection 4.4. Explicit expressions for the other cycle statistics in Prop. 1 will be provided in Subsection 5.3.

It may seem surprising that we do not need to subdivide the calculation into the component from the N_c complete cycles and the terminal cycle, since the probability distribution of the attachment jump $\widetilde{\Delta M}_{J^{(d)'}}^{(a)}$, does depend on whether it is a terminal cycle. But Wald's identity precisely allows us to do this because, viewed jointly, the sequence of times taken, cargo motion incurred (including the jump variables), and attachment/detachment events within each cycle are independent and identically distributed across cycles. It is only when one conditions on the first cycle that leads to complete detachment (N_c + 1) that the cargo motion incurred on each cycle is no longer identically distributed. Our calculation involving Wald's identity eschews this conditioning step, which in fact would further complicate the calculation due to its effect on which motor $J^{(d)}$ detaches during a cycle (see Subsection 5.3 below).

5.2 Effective velocity and diffusion

The characterization of the effective velocity and diffusivity is not so straightforward for a motor-cargo complex that eventually detaches from a microtubule. One cannot directly take the long-time limit of the ratio of distance traveled to time, since the motor-cargo complex will detach at a finite time. Of course, for cooperative motor models that explicitly model a rate for reattachment for the motors even from the fully detached state, one can define an effective velocity and diffusivity in the usual way, essentially averaging progress over both phases where the motor-cargo complex is attached or detached from a microtubule [23,31,82]. While such an effective velocity is meaningful for characterizing transport, it

does not relate so naturally to experimental observations of particular cargo, which are tracked only while they appear to be attached to a microtubule. Moreover, the time until reattachment could be quite long. In a model with explicit reattachment from the fully detached state, one could alternatively and meaningfully define a effective velocity conditioned on attachment [13], but it is not clear how to similarly define a diffusivity conditioned on attachment.

In order to describe the effective velocity and diffusivity of cargo during periods where at least one of its motors is attached to a microtubule, we consider two distinct definitions of effective velocity and diffusivity which could be applied to any theoretical or simulation model for motor-cargo dynamics, without reference to a model for reattachment from a state of complete detachment:

1. Pooling run times $T^{(j)}$ and run lengths $L^{(j)}$ over independent experiments $j = 1, \ldots, S$, and defining the ensemble velocity and diffusivity as:

$$V_{\text{ens}} \equiv \lim_{S\to\infty} \frac{\sum_{j=1}^{S} L^{(j)}}{\sum_{j=1}^{S} T^{(j)}}, \tag{70}$$

$$D_{\text{ens}} \equiv \lim_{S\to\infty} \frac{\sum_{j=1}^{S} \left(L^{(j)} - V_{\text{ens}} T^{(j)}\right)^2}{2\sum_{j=1}^{S} T^{(j)}}. \tag{71}$$

2. We may alternatively censor experiments by requiring that they complete a certain number of full cycles, thereby defining the long-run velocity and diffusivity as

$$V_{\text{run}} \equiv \lim_{k\to\infty} \lim_{S\to\infty} \frac{\sum_{j=1}^{S} L^{(j)} \mathbf{1}_{N_c^{(j)} > k}}{\sum_{j=1}^{S} T^{(j)} \mathbf{1}_{N_c^{(j)} > k}}, \tag{72}$$

$$D_{\text{run}} \equiv \lim_{k\to\infty} \lim_{S\to\infty} \frac{\sum_{j=1}^{S} \left((L^{(j)} - V_{\text{run}} T^{(j)}) \mathbf{1}_{N_c^{(j)} > k}\right)^2}{2\sum_{j=1}^{S} T^{(j)} \mathbf{1}_{N_c^{(j)} > k}}. \tag{73}$$

What we have defined as the ensemble velocity should coincide with the velocity conditioned on attachment in models with explicit reattachment from a completely detached state [13]. With regard to the distinction in the definition of the long-run transport statistics, note that a large number of cycles during a run, $N_c^{(j)} \to \infty$, implies (almost surely) a large run time $T^{(j)} \to \infty$. The idea here is that one may often only wish to take data on sufficiently long runs in experiments, or simulations, in order to downplay transient effects at the beginning or end of a cargo run, and better characterize the dynamics in the middle of a run. Censoring on run time $T^{(j)}$ rather than the number of attachment/detachment cycles $N_c^{(j)}$ in a simulation or experiment would be more natural, but the derivation of the theoretical

expression would be less straightforward, so we leave its consideration for a later work. The $k \to \infty$ limit is the more important one in the above definitions as it characterizes a "long run". The $S \to \infty$ limit of many experiments passing the censoring step is unnecessary for computing the long-run velocity and only needed for computing the long-run diffusivity since we only take data on the total time and displacement of a run. We have left aside here the capacity, often exploited, to use observations of the cargo position at intermediate times within a run to infer velocity or diffusivity through, for example, fitting mean displacement and mean-squared displacement as a function of time [83,84,18]. More complex statistical definitions of measured velocity and diffusivity could be accordingly formulated. We finally remark that in the limit of small detachment rate, the long-run statistics should converge to the ensemble transport statistics since most runs will be long [85].

The ensemble definition has good mathematical properties and is an idealized manner of estimating velocity and diffusivity in experiments, but we must bear in mind that experiments typically only measure runs of a cargo that are sufficiently long [86,69,56,32], since short runs are difficult to detect or disambiguate from noise. Thus, the actual experimental values might fall somewhere between the ensemble and long-run definitions given above, so we will study both. The selection of runs to record in an experiment can be censored in other ways as well, for example those with an observable initial attachment and complete detachment event [87].

Some stochastic simulations also compute velocity (and sometimes diffusivity) using the ensemble definitions given above [88], though some simulation studies compute velocities and diffusivities in each run, and then average the single-run velocities and diffusivities over the ensemble [68,26] by averaging the ratio of run length to run time ($\frac{1}{S}\sum_{j=1}^{S}\frac{L(j)}{T(j)}$). The latter has no inherent connection to long-time properties, but would be approximated by the long-run definitions if the run times happened to be sufficiently long in some statistical sense [85]. This velocity estimator, however, has infinite variance [85] while the ensemble definition (71) (with a large but finite number of samples S) enjoys the good statistical convergence properties afforded by the applicability of the central limit theorem.

We define $\mathscr{A}$ as the event that a cycle ends with a return to the two-motor-attached state ($(1,2) \to (i) \to (1,2)$) rather than to the detachment of the complex ($(1,2) \to (i) \to 0$). The formulas for the long-run velocity and diffusivity involve first and second moment statistics of cycle displacements and durations, conditioned upon $\mathscr{A}$; we denote these conditional statistics by appending "$|\mathscr{A}$" in the subscript. As $N_c \to \infty$, the contribution of the terminal cycles in V_{run} and D_{run} become negligible. From the standard law of large numbers for independent random variables for the case of ensemble statistics, and its version for renewal-reward processes [89,90] for the long-run statistics, we arrive at the following expressions:

Proposition 2 *(Velocity and diffusivity from cycle statistics) If all runs are initialized from a state in which both motors are attached:*

1. *The ensemble velocities and diffusivity are given by*

$$V_{\text{ens}} = \frac{\boldsymbol{\mu}_L}{\boldsymbol{\mu}_T} = \frac{\boldsymbol{\mu}_{\Delta M_c}}{\boldsymbol{\mu}_{\Delta T_c}}, \tag{74}$$

$$\begin{aligned} D_{\text{ens}} &= \frac{V_{\text{ens}}^2 \boldsymbol{\sigma}_T^2 + \boldsymbol{\sigma}_L^2 - 2V_{\text{ens}} \boldsymbol{\sigma}_{T,L}}{2\boldsymbol{\mu}_T} \\ &= \frac{V_{\text{ens}}^2 \boldsymbol{\sigma}_{\Delta T_c}^2 + \boldsymbol{\sigma}_{\Delta M_c}^2 - 2V_{\text{ens}} \boldsymbol{\sigma}_{\Delta T_c, \Delta M_c}}{2\boldsymbol{\mu}_{\Delta T_c}}. \end{aligned} \tag{75}$$

2. *The long-run velocity and diffusivity are given by*

$$V_{\text{run}} = \frac{\boldsymbol{\mu}_{\Delta M_c \mid \mathscr{A}}}{\boldsymbol{\mu}_{\Delta T_c \mid \mathscr{A}}}, \tag{76}$$

$$\begin{aligned} D_{\text{run}} &= \frac{1}{2}\left(\frac{\boldsymbol{\mu}_{\Delta M_c \mid \mathscr{A}}^2 \boldsymbol{\sigma}_{\Delta T_c \mid \mathscr{A}}^2}{\boldsymbol{\mu}_{\Delta T_c \mid \mathscr{A}}^3} + \frac{\boldsymbol{\sigma}_{\Delta M_c \mid \mathscr{A}}^2}{\boldsymbol{\mu}_{\Delta T_c \mid \mathscr{A}}} - \frac{2\boldsymbol{\mu}_{\Delta M_c \mid \mathscr{A}} \boldsymbol{\sigma}_{\Delta M, \Delta T \mid \mathscr{A}}}{\boldsymbol{\mu}_{\Delta T_c \mid \mathscr{A}}^2} \right) \\ &= \frac{V_{\text{run}}^2 \boldsymbol{\sigma}_{\Delta T_c \mid \mathscr{A}}^2 + \boldsymbol{\sigma}_{\Delta M_c \mid \mathscr{A}}^2 - 2V_{\text{run}} \boldsymbol{\sigma}_{\Delta M, \Delta T \mid \mathscr{A}}}{2\boldsymbol{\mu}_{\Delta T_c \mid \mathscr{A}}}. \end{aligned} \tag{77}$$

We see that the expressions for the ensemble and long-run velocity and diffusivity in terms of cycle statistics have a similar structure, with the latter involving a conditioning on the cycle indeed returning to a state of two attached motors rather than possibly terminating in complete detachment.

Corollary 1 *When the two motors in the ensemble have identical parameters, then* $V_{\text{ens}} = V_{\text{run}}$ *and*

$$| D_{\text{ens}} - D_{\text{run}} | \leq \frac{1}{8\boldsymbol{\mu}_{\Delta T_c}}.$$

We prove this corollary in Subsection 5.3.3. For both kinesin-1/kinesin-1 and kinesin-2/kinesin-2 ensembles which we consider in Section 6, the difference in diffusivities is less than one percent. The distinction between ensemble and long-run transport characteristics therefore appear potentially important mainly for heterogenous ensembles.

5.3 Expressions for cycle statistics

The formulas for the effective motor-cargo transport in Subsections 5.1 and 5.2 refer to statistics of durations and displacements within detachment-attachment cycles. We now provide formulas for these cycle statistics, followed by a discussion of how they are derived.

Proposition 3 *(Explicit expressions of cycle statistics)*

1. *The first and second order moments of the unconditional cycle times and displacements have the explicit forms in terms of the effective nondimensional parameters defined in the coarse-grained model from* Section 4:

$$\boldsymbol{\mu}_{\Delta T_c} = \frac{1}{\bar{d}^*_{1,2}} + \frac{p_d^{(2)}}{\bar{a}^{*(2)} + \bar{d}^*_1} + \frac{p_d^{(1)}}{\bar{a}^{*(1)} + \bar{d}^*_2}, \tag{78}$$

$$\begin{aligned}\boldsymbol{\mu}_{\Delta M_c} = {} & \frac{V_{1,2}}{\bar{d}^*_{1,2}} + \frac{1}{2}\left(\boldsymbol{\mu}_{R_2^{(d)}} p_d^{(2)} \widetilde{\boldsymbol{\kappa}}^{(2)} - \mu_{R_1^{(d)}} p_d^{(1)} \widetilde{\boldsymbol{\kappa}}^{(1)}\right) + \frac{p_d^{(2)} V_1}{\bar{a}^{*(2)} + \bar{d}^*_1} \\ & + \frac{p_d^{(1)} V_2}{\bar{a}^{*(1)} + \bar{d}^*_2} - \frac{\widetilde{F}_T}{2}\left(p_d^{(2)} \frac{\widetilde{\boldsymbol{\kappa}}^{(2)}}{\widetilde{\boldsymbol{\kappa}}^{(1)}} + p_d^{(1)} \frac{\widetilde{\boldsymbol{\kappa}}^{(1)}}{\widetilde{\boldsymbol{\kappa}}^{(2)}}\right),\end{aligned} \tag{79}$$

$$\begin{aligned}\boldsymbol{\sigma}^2_{\Delta T_c} = {} & \frac{1}{(\bar{d}^*_{1,2})^2} + \frac{p_d^{(2)}}{(\bar{a}^{*(2)} + \bar{d}^*_1)^2} + \frac{p_d^{(1)}}{(\bar{a}^{*(1)} + \bar{d}^*_2)^2} \\ & + p_d^{(2)} p_d^{(1)} \left(\frac{1}{\bar{a}^{*(2)} + \bar{d}^*_1} - \frac{1}{\bar{a}^{*(1)} + \bar{d}^*_2}\right)^2,\end{aligned} \tag{80}$$

$$\begin{aligned}\boldsymbol{\sigma}^2_{\Delta M_c} = {} & \frac{2D_{1,2}}{\bar{d}^*_{1,2}} + \left(\frac{V_{1,2}}{\bar{d}^*_{1,2}}\right)^2 \\ & + \sum_{i=1}^{2} p_d^{(i)} \left(\frac{2D_{i'}}{\bar{a}^{*(i)} + \bar{d}^*_{i'}} + \left(\frac{V_{i'}}{\bar{a}^{*(i)} + \bar{d}^*_{i'}}\right)^2 + \frac{1 - p_d^{\varnothing}}{4} \frac{\widetilde{\boldsymbol{\kappa}}^{(i)}}{\widetilde{\boldsymbol{\kappa}}^{(i')}} + \frac{1}{4}(\widetilde{\boldsymbol{\kappa}}^{(i)})^2 \boldsymbol{\sigma}^2_{R_i^{(d)}}\right) \\ & + p_d^{(1)} p_d^{(2)} \left(\left(\frac{\widetilde{\boldsymbol{\kappa}}^{(1)} - \widetilde{\boldsymbol{\kappa}}^{(2)}}{\widetilde{\boldsymbol{\kappa}}^{(1)} \widetilde{\boldsymbol{\kappa}}^{(2)}}\right) \widetilde{F} + \sum_{i=1}^{2} \left(\frac{(-1)^{i+1} V_i}{\bar{a}^{*(i')} + \bar{d}^*_i} + \frac{\boldsymbol{\mu}_{R_i^{(d)}} \widetilde{\boldsymbol{\kappa}}^{(i)}}{2}\right)\right)^2,\end{aligned} \tag{81}$$

$$\begin{aligned}\boldsymbol{\sigma}_{\Delta T_c, \Delta M_c} = {} & \frac{V_{1,2}}{(\bar{d}^*_{1,2})^2} + \frac{p_d^{(2)} V_1}{(\bar{a}^{*(2)} + \bar{d}^*_1)^2} + \frac{p_d^{(1)} V_2}{(\bar{a}^{*(1)} + \bar{d}^*_2)^2} \\ & + p_d^{(1)} p_d^{(2)} \left(\frac{1}{\bar{a}^{*(2)} + \bar{d}^*_1} - \frac{1}{\bar{a}^{*(1)} + \bar{d}^*_2}\right) \\ & \times \left(\left(\frac{\widetilde{\boldsymbol{\kappa}}^{(1)} - \widetilde{\boldsymbol{\kappa}}^{(2)}}{\widetilde{\boldsymbol{\kappa}}^{(1)} \widetilde{\boldsymbol{\kappa}}^{(2)}}\right) \widetilde{F} + \sum_{i=1}^{2} \left(\frac{(-1)^{i+1} V_i}{\bar{a}^{*(i')} + \bar{d}^*_i} + \frac{\boldsymbol{\mu}_{R_i^{(d)}} \widetilde{\boldsymbol{\kappa}}^{(i)}}{2}\right)\right).\end{aligned} \tag{82}$$

Additional notation used here is $i' = 3 - i$ *(the index of the "other" motor), the probability* $p_d^{(i)} = \frac{\bar{d}^{*(i)}_{1,2}}{\bar{d}^*_{1,2}}$ (50) *that motor i detaches first from the state of both motors attached, the unconditional probability of complete detachment in a given*

cycle $p_d^{\varnothing}$ (57), *and* $\mu_{R_i}^{(d)}$, *the conditional mean of* $R^{(\mathrm{d})}$ *given detachment of motor i, which may be computed from its probability density* (51).

2. *Expressions of the corresponding cycle statistics which are conditioned on* $\mathscr{A}$, *the cycle being complete and returning to a state of two motors attached, are the same as corresponding statistics given in the above* equations (79)-(83), *except that*

   a. *In all instances,* $p_d^{(i)}$ *is replaced with*

$$p_{d\,|\,\mathscr{A}}^{(i)} = \left(1 + \frac{\bar{a}^{(i')}}{\bar{a}^{(i)}} \frac{\bar{d}_{1,2}^{*\,(i')}}{\bar{d}_{1,2}^{*\,(i)}} \frac{\bar{d}_{i'}^{*} + \bar{a}^{(i)}}{\bar{d}_{i}^{*} + \bar{a}^{(i')}}\right)^{-1}. \tag{83}$$

   b. *To compute* $\sigma_{\Delta M_{\mathrm{c}}\,|\,\mathscr{A}}$, *in* equation (82) *we replace the term* $p_d^{\varnothing}$ *(defined in* (57)) *with 0.*

5.3.1 Derivation of unconditional cycle statistics in Proposition 3—We begin by computing statistics for run lengths and times for different attachment states involved in a cycle. For evolution with two attached motors, we invoke the law of total expectation, conditioning on $\Delta T_{1,2}$, to obtain

$$\mathbb{E}[\Delta M_{1,2}] = \frac{V_{1,2}}{\bar{d}_{1,2}^{*}}. \tag{84}$$

From (61), we may use the law of total variance, to obtain

$$Var(\Delta M_{1,2}) = \frac{2D_{1,2}}{\bar{d}_{1,2}^{*}} + \left(\frac{V_{1,2}}{\bar{d}_{1,2}^{*}}\right)^2. \tag{85}$$

Next, from the definition (60) of ΔM_{c} we obtain, by conditioning on possible values of $J^{(d)}$,

$$\begin{aligned}\boldsymbol{\mu}_{\Delta M_{\mathrm{c}}} = \frac{V_{1,2}}{\bar{d}_{1,2}^{*}} &+ p_d^{(2)}\left(\frac{V_1}{\bar{a}^{*\,(2)} + \bar{d}_1^{*}} + \frac{\widetilde{\boldsymbol{\kappa}}^{(2)}\boldsymbol{\mu}_{R_2^{(d)}}}{2} - \frac{\widetilde{\boldsymbol{\kappa}}^{(2)}\widetilde{F}_T}{2\widetilde{\boldsymbol{\kappa}}^{(1)}}\right) \\ &+ p_d^{(1)}\left(\frac{V_2}{\bar{a}^{*\,(1)} + \bar{d}_2^{*}} - \frac{\widetilde{\boldsymbol{\kappa}}^{(1)}\boldsymbol{\mu}_{R_1^{(d)}}}{2} - \frac{\widetilde{\boldsymbol{\kappa}}^{(1)}\widetilde{F}_T}{2\widetilde{\boldsymbol{\kappa}}^{(2)}}\right),\end{aligned} \tag{86}$$

which is equivalent to (80). A similar argument, referring to Eq. (58) and (59) yields (79).

From (52), (56), and (27) we can similarly compute the following statistics:

$$\mathbb{E}(\Delta M_i) = \frac{V_i}{\bar{a}^{*(i')} + \bar{d}_i^*}, \qquad Var(\Delta M_i) = \frac{2D_i}{\bar{a}^{*(i')} + \bar{d}_i^*} + \left(\frac{V_i}{\bar{a}^{*(i')} + \bar{d}_i^*}\right)^2,$$
$$\mathbb{E}(\Delta M_i^{(\mathrm{a})}) = 0, \qquad Var(\Delta M_i^{(\mathrm{a})}) = \frac{1}{4}\frac{\widetilde{\boldsymbol{\kappa}}^{(i)}}{\widetilde{\boldsymbol{\kappa}}^{(i')}}, \tag{87}$$

$$\mathbb{E}(\widetilde{\Delta M}_i^{(\mathrm{a})}) = 0, \qquad Var(\widetilde{\Delta M}_i^{(\mathrm{a})}) = \frac{1 - p_d^{\varnothing}}{4}\frac{\widetilde{\boldsymbol{\kappa}}^{(i)}}{\widetilde{\boldsymbol{\kappa}}^{(i')}}, \tag{88}$$

$$\mathbb{E}(\Delta M_i^{(\mathrm{d})}) = \frac{\widetilde{\boldsymbol{\kappa}}^{(i)}}{2}\left((-1)^i \boldsymbol{\mu}_{R_i^{(d)}} - \frac{\widetilde{F}}{\widetilde{\boldsymbol{\kappa}}^{(i')}}\right), \quad Var(\Delta M_i^{(\mathrm{d})}) = \frac{1}{4}(\widetilde{\boldsymbol{\kappa}}^{(i)})^2 \sigma^2_{R_i^{(d)}}. \tag{89}$$

Here, we note that the mean $\mu_{R_i^{(d)}}$ and variance $\sigma^2_{R_i^{(d)}}$ of the intermotor separation $R_i^{(d)}$ at the detachment time, given motor i detaches first, may be computed directly from the density given in Eq. (51). For the special case of constant detachment rates, $\mu_{R_i^{(d)}} = \mu_R$ and $\sigma_{R_i^{(d)}} = \sigma_R$.

To find $\sigma^2_{\Delta T_{\mathrm{c}}}$ and $\sigma^2_{\Delta M_{\mathrm{c}}}$, observe that the times spent and dynamics within the fully attached and one-motor detached states are independent, which implies

$$\boldsymbol{\sigma}^2_{\Delta T_{\mathrm{c}}} = Var(\Delta T_{1,2}) + Var(\Delta T_{\boldsymbol{J}^{(d)'}}),$$
$$\boldsymbol{\sigma}^2_{\Delta M_{\mathrm{c}}} = Var(\Delta M_{1,2}) + Var(\Delta M_{\boldsymbol{J}^{(d)'}} + \widetilde{\Delta M}^{(\mathrm{a})}_{\boldsymbol{J}^{(d)}} + \Delta M^{(\mathrm{d})}_{\boldsymbol{J}^{(d)}}). \tag{90}$$

From (59), $Var(\Delta T_{1,2}) = 1 / (\bar{d}^*_{1,2})^2$. For the second term in (91), we use the law of total variance, conditioning on $\boldsymbol{J}^{(d)}$, to obtain

$$Var(\Delta T_{\boldsymbol{J}^{(d)'}}) = Var(\Delta T_1) p_d^{(2)} + Var(\Delta T_2) p_d^{(1)} + (\mathbb{E}[\Delta T_1 - \Delta T_2])^2 p_d^{(2)} p_d^{(1)},$$

which, using (59), yields (81). A similar calculation gives (82), with attachment and detachment jumps, due to their association with the fast dynamics of the cargo and detached motors, taken as independent of each other and of the progress of the cargo tracking variable during the time one motor was attached.

It remains to calculate the covariance $\sigma_{\Delta T_{\mathrm{c}}, \Delta M_{\mathrm{c}}}$, which may be decomposed as the sum

$$\sigma_{\Delta T_c, \Delta M_c} = \mathrm{Cov}(\Delta M_{1,2}, \Delta T_{1,2}) + \mathrm{Cov}(\Delta M_{J^{(d)'}} + \widetilde{\Delta M}^{(a)}_{J^{(d)}} + \Delta M^{(d)}_{J^{(d)}}, \Delta T_{J^{(d)'}}) \tag{91}$$

The first term follows easily from the law of total covariance, conditioning on $\Delta T_{1,2}$:

$$\mathrm{Cov}(\Delta T_{1,2}, \Delta M_{1,2}) = \frac{V_{1,2}}{(\bar{d}^*_{1,2})^2}, \tag{92}$$

Through another application of the law of total covariance, conditioning on $J^{(d)}$ and noting the conditional independence of the jumps in the cargo tracking variable $\widetilde{\Delta M}^{(a)}_{J^{(d)}}$ and $\Delta M^{(d)}_{J^{(d)}}$ from the residence times $\Delta T_{J^{(d)'}}$, we may write

$$\begin{aligned}
&\mathrm{Cov}(\Delta M_{J^{(d)'}} + \widetilde{\Delta M}^{(a)}_{J^{(d)}} + \Delta M^{(d)}_{J^{(d)}}, \Delta T_{J^{(d)'}}) \\
&= p_d^{(2)} \mathrm{Cov}(\Delta M_1, \Delta T_1) + p_d^{(1)} \mathrm{Cov}(\Delta M_2, \Delta T_2) \\
&+ p_d^{(1)} p_d^{(2)} (\mathbb{E}[\Delta T_1] - \mathbb{E}[\Delta T_2]) \\
&\times (\mathbb{E}[\Delta M_1 + \widetilde{\Delta M}^{(a)}_2 + \Delta M^{(d)}_2] - \mathbb{E}[\Delta M_2 + \widetilde{\Delta M}^{(a)}_1 + \Delta M^{(d)}_1]).
\end{aligned}$$

A direct calculation of each of these terms yields (83).

5.3.2 Derivation of conditional cycle statistics in Proposition 3—By the independence of residence time of a state and the next state in a continuous-time Markov chain, the conditioning upon re-entry into the state of two attached motors does not affect distributions of attachment and detachment times given in (59), nor the components of the cargo-tracking displacements $\Delta M_{1,2}$, ΔM_i, $\Delta M^{(a)}_i$, and $\Delta M^{(d)}_i$. What is affected is the probability distribution of which motor is the one to detach from the state of two attached motors.

Let $J^{(d)} \mid \mathscr{A}$ denote the index of the motor which detaches during a cycle, conditioned on the event $\mathscr{A}$ of next returning to a two-motor attached state rather than to a state of complete detachment. We can compute the distribution of $J^{(d)} \mid \mathscr{A}$ through Bayes' rule, with

$$\begin{aligned}
p^{(i)}_{d \mid \mathscr{A}} &:= \mathbb{P}(J^{(d)} = i \mid \mathscr{A}) \\
&= \mathbb{P}(\mathscr{A} \mid J^{(d)} = i) \frac{\mathbb{P}(J^{(d)} = i)}{\mathbb{P}(\mathscr{A})} = \frac{\dfrac{\bar{a}^{(i)}}{\bar{d}^*_{i'} + \bar{a}^{(i)}} \left(\dfrac{\bar{d}^{*(i)}_{1,2}}{\bar{d}^*_{1,2}} \right)}{\dfrac{\bar{a}^{(i)}}{\bar{d}^*_{i'} + \bar{a}^{(i)}} \left(\dfrac{\bar{d}^{*(i)}_{1,2}}{\bar{d}^*_{1,2}} \right) + \dfrac{\bar{a}^{(i')}}{\bar{d}^*_{i} + \bar{a}^{(i')}} \left(\dfrac{\bar{d}^{*(i')}_{1,2}}{\bar{d}^*_{1,2}} \right)} \\
&= \left(1 + \frac{\bar{a}^{(i')}}{\bar{a}^{(i)}} \frac{\bar{d}^{*(i')}_{1,2}}{\bar{d}^{*(i)}_{1,2}} \frac{\bar{d}^*_{i'} + \bar{a}^{(i)}}{\bar{d}^*_{i} + \bar{a}^{(i')}} \right)^{-1}.
\end{aligned}$$

Note the conditioning on returning to the state of two attached motors biases the probability distribution for which motor detaches toward the one that is more likely to reattach.

When conditionining ΔM_c on the event $\mathscr{A}$, the only variables affected are $J^{(d)}$ and $\widetilde{\Delta M}^{(a)}_{J^{(d)}}$). Thus, expressions in (79)-(83) now are computed with $\mathbb{P}(J^{(d)} = i \mid \mathscr{A}) = p^{(i)}_{d \mid \mathscr{A}}$ rather than $p^{(i)}_d$. To obtain $\sigma_{\Delta M_c \mid \mathscr{A}}$, we note that $\widetilde{\Delta M}^{(a)}_{J^{(d)}} \mid \mathscr{A} \sim \Delta M^{(a)}_{J^{(d)} \mid \mathscr{A}}$, and carry out calculations similar to those which yield (82).

5.3.3 Derivation of special case of identical motors in Corollary 1—From these formulas, we observe that if two motors in an ensemble have identical parameters, it follows from symmetry that $p^{(1)}_d = p^{(1)}_{d \mid \mathscr{A}} = 1/2$, and consequently $V_{ens} = V_{run}$. Effective diffusivities D_{ens} and D_{run} for identical motors ensembles are, in general, not equal due to the difference in the term involving $p^{\varnothing}_d$ in equation (82). However, a straightforward estimate comparing the effect of this term on (76) and (78) shows that the diffusivities differ at most by $1/(8\mu_{\Delta T_c})$.

6 Simulations

In this section, we compare theoretical and sample statistics through direct simulation of equations (1)-(4) for two motor ensembles. Both homogeneous (kinesin-1/kinesin-1 or kinesin-2/kinesin-2) and heterogeneous (kinesin-1/kinesin-2) ensembles are simulated, using the parameters in Table 1. For each ensemble, we consider optical trap forces of $F_T = -5,0,$and 5 pN. We also considered two separate detachment models. The first utilizes the double exponential function given in (8). For comparison, we also use a constant detachment rate set equal to the average of the double-exponential detachment rate model against the stationary distribution of the force F applied by the cargo when the motor in question is the only one attached with no trap force. Therefore, at zero trap force, both models have the same nondimensional effective detachment rates $\bar{d}^*_i$, but the first model has a double exponential function describing the detachment rate as a function of force while the second model has a force-independent detachment rate. Note that, for the constant detachment rate case, this would also be the detachment rate from the state with two motors attached, but would in general differ from the effective detachment rate $\bar{d}^{*(i)}_{1,2}$ (43) for the double-exponential detachment rate model. The effective detachment rates from the state of one motor attached will be higher under assisting or opposing trap forces for the double-exponential detachment rate model relative to the constant detachment rate model. In all cases, we used constant values $a^{(i)}$ for attachment rates. Values of parameters related to attachment and detachment are found in Table 1.

The stochastic differential equations (1)-(2) were simulated by an Euler-Maruyama discretization with a time increment $\Delta t = 10^{-6}$s. The random switching was discretized with respect to the same time interval, with probabilities to switch as the momentary rate multiplied by the time step. For stability and accuracy concerns, the time step was selected to be less than the time scale γ_m/κ for the drift of unattached motors (and consequently the

larger time scales for attached motors, cargo, and switching dynamics). Our choice of the nondimensional force-velocity curve g in Eq. (4) is the same used in McKinley, Athreya, et al [34], defined by

$$g(x) = A - B\tanh(Cx - D), \tag{93}$$

with $g(x) \to 1.2$ as $x \to -\infty$ and $g(x) \to -.1$ as $x \to \infty$. With the requirements $g(0) = 1$ and $g(1) = 0$, the constants A, B, C, and D may be uniquely determined numerically.

We show a sample path of motor and cargo positions in Fig. 4 near times of attachment and detachment at zero trap force $F_T = 0$. As predicted by the calculation (28) (or the force balance analysis of [13,24]), the mean cargo position is a weighted average of the position of kinesin-1 and kinesin-2 when both motors are attached. When one motor is attached, the detached motor and cargo both have mean position equal to the current position of the attached motor. Fig. 4 also suggests that the transient period for motors and cargo to change their relative positions is small compared to times between attachment or detachment. In particular, we can interpret the jumps in the cargo position at motor detachment events as potentially corresponding to "flyback" seen in experimental traces [91,50,14].

For each combination of motor ensemble (kinesin-1/kinesin-1, kinesin-2/kinesin-2, or kinesin-1/kinesin-2), detachment model (constant or double exponential), and trap force strength ($F_T = -5$, 0, or 5 pN), we simulated $S = 2{,}000$ runs, each beginning with two attached motors and cargo at identical positions along the microtubule, and terminating with complete detachment from the microtubule. All experiments have the same initial conditions $X_1(0) = X_2(0) = Z(0) = 0$. However, due to repositioning from force balance, we should expect the cargo to quickly readjust to 10 nm for $F_T = -5$ pN and to −10 nm for $F_T = 5$ pN. We include these corrections in reporting our simulation results. Table 3 reports these simulation results for constant detachment rates and Table 4 for double exponential detachment rate functions. For the means of run times T, run lengths L, and number of cycles N_c, estimates are given by sample means with intervals of the standard error. The ensemble velocities and diffusions are estimated using the finite $S = 2{,}000$ version of the formulas (71) and (72), with errors estimated from bootstrapping. Specifically, from our data $\Theta = (T^{(j)}, L^{(j)})_{j=1,\ldots,S}$ for the run times and run lengths in the $S = 2{,}000$ simulations, we drew $B = 1{,}000$ bootstrap samples $\boldsymbol{\Theta}_b^* = (T_b^{(j)}, L_b^{(j)})_{j=1,\ldots,S}$, for each $b = 1, \ldots, B$, where each $(T_b^{(j)}, L_b^{(j)})$ denotes a random sample *with replacement* from Θ. For V_{run} (73) and D_{run} (74), we use a similar procedure, with now the dataset Θ thinned to those $S/10 = 200$ data pairs associated to the run lengths $L^{(j)}$ in the top decile.

Our main concern here will be the question of adequacy of the theoretical results based on the asymptotic analysis relative to the Monte Carlo simulations, but we first remark on how the velocities, both theoretical and simulated, can be quite a bit faster than either of the kinesin-1 or kinesin-2 maximum speeds when the trap force is assisting ($F_T = -5$pN). Note first that under our force-velocity model (94), the motors can move 20% faster than their unloaded speeds, listed in Table 1, under assisting loads. The reason the reported effective velocities can exceed even this figure is the contribution from the jumps in the cargo tracking variable at detachment events (Subsubsection 4.3.2). Indeed, the cargo with no

motors bound will travel under an assisting force at an average speed $F_T/\gamma \sim 5 \times 10^5$nm/s. Of course we are only considering the cargo during times where one of the associated motors is attached to a microtubule, but this indicates the cargo can move considerably more quickly than the motor speeds when one motor detaches. So what is really causing these large velocities under assisting forces is typically that the lagging motor (under stronger force and therefore higher detachment rate since the cargo is typically ahead of the motors under assisting force) detaches, freeing the cargo to quickly move forward to the new quasi-equilibrium with the remaining attached motor, and meanwhile the detached motor also quickly moves up to the cargo's position and reattaches near the cargo's new position, becoming now the leading motor. These jumpy adjustments can allow the cargo to move at a large velocity, at least until the cycle is broken by the attached motor detaching before the detached motor reattaches.

Returning to the central question of the adequacy of the theoretical asymptotic approximation, we see from Table 3 that the simulations well support the theoretical approximations for models with constant detachment rates. The diffusivities are somewhat underestimated for hindering trap forces, and overestimated for the kinesin-1/kinesin-2 ensemble at zero trap force. These issues carry over to the double exponential detachment rate model in Table 4, with now a substantial overestimation of diffusivity for the kinesin-1/kinesin-2 ensemble with assisting trap force. These discrepancies can be traced to order of magnitude errors in some of the second moment cycle statistics (Eqs. (81) through (83)), which are apparently more sensitive to the non-ideal scale separation.

A more fundamental discrepancy emerges for the kinesin-2/kinesin-2 ensemble with hindering trap force, where the mean run length but not the mean run time is overestimated by a factor of two by the theory, and the velocity similarly overestimated. What appears to make this case the most problematic for the theory is the failure of the assumption that detachment from the state (1,2) with both motors attached takes place on a time scale long compared with that required for the intermotor separation R to reach its stationary distribution (34). First of all, the nondimensional effective rate of detachment from this state, $\bar{d}^*_{1,2} = 0.24$, is the highest for this case out of all considered, and is therefore the least well separated from the $ord(1)$ time scale of the relaxation dynamics of the intermotor separation R. Moreover, the force scale of detachment under hindering forces (for both kinesin-1 and kinesin-2) is about $F_{d+} = 2$pN (Table 1), which is on the order of the load carried by each motor under a trap force of 5 pN. Upon reattachment from the state of one attached motor, the leading motor will still be carrying approximately 5 pN of load, since the recently reattached motor is typically near the cargo position and relaxed, and so the leading motor will be considerably more likely to detach shortly after reattachment than it would under an averaged theory where both motors are carrying 2.5 pN of load on average. Kinesin-1 is similarly sensitive to fluctuations in hindering load, but its lower base rate of detachment d_{0+} appears not to lead to a substantial violation of the scale separation assumption (Table 1).

7 Discussion and Conclusions

7.1 Summary and Related Work

We have developed and analyzed a mathematical model for the transport of cargo by multiple, nonidentical molecular motors along a microtubule. The spatial dynamics are formulated in terms of stochastic differential equations, coarse-graining implicitly over the stepping dynamics of the motors. The process of detachment is modeled via a Cox process, in that the detachment rate depends on the spatial configuration of the motor-cargo complex, which in turn is a random process governed by the stochastic differential equations. Nondimensionalization revealed an at least nominal separation of time scales between detached motor dynamics, cargo dynamics, attached motor dynamics, and attachment/detachment processes. For the case of two motors attached to a cargo, we exploited this scale separation by successive averaging and homogenization procedures to arrive at an effective continuous-time Markov chain for the attachment states of the two motors, together with random displacements of a cargo tracking variable associated with each visit to a state. The cargo tracking variable is just a smoothed representation of the position of the cargo that has the same long-time dynamics. The displacements of this cargo tracking variable in each state also include jumps associated with attachment and detachment events where the cargo tracking variable adjusts, on a fast time scale, to the new state. We developed analytical formulas for the effective velocity, diffusivity, and processivity of the cargo by an application of the law of large numbers and renewal-reward asymptotics to a decomposition of the coarse-grained Markov chain into regeneration cycles. [1].

Miles, Lawley, and Keener [31] previously pursued in a similar spirit an analysis of effective transport and processivity of a cargo with multiple motors attached via renewal reward theory. Their procedure, as ours, relies on a separation of time scales between the continuous dynamics of spatial motion of the motors and cargo and the attachment and detachment kinetics. Our use of the cargo tracking variable in Subsection 4.1 to provide a representation of the cargo position even when it has been explicitly removed as a fast variable is similar in spirit to the study in [31] of the conditional expectation of the cargo (and motor) variables given the attachment/detachment state of the motors. While our methods of analysis share these similarities with [31], our model and analysis does offer several complements. First of all, we remark that [31] start with a stepping model for the motors, while we opted for a coarse-grained stochastic differential equation to unify the mathematical description with the cargo dynamics. We note below that our approach could be extended to motor stepping models, and we intend to do this in future work. Our model, on the other hand, has the following distinctive features relative to the model of [31]: First, we allow the motors to be of different types, since we are interested in understanding dynamics of heterogenous ensembles as studied for example in Feng, Mickolajczyk, et al [14]. [31] was rather motivated to explain the emergence of transport ability of homogenous collections of the non-processive motor Ncd [32]. Secondly, we model motor dynamics and detachment rates in terms of the instantaneous force felt and thus the spatial configuration. [31] rather model

[1]This latter procedure is presented in more generality in a separate publication “Renewal reward perspective on linear switching diffusion systems in models of intracellular transport” by M. V Ciocanel, J. Fricks, P. R. Kramer, and S. A. McKinley

motor dynamics and detachment in terms of the number of currently attached motors, which could be viewed as a phenomenological way of accounting for the different distributions of forces experienced, but this framework does not adapt well to mixed motor types. Third, we provide a statistical model for the detached motors and where they reattach, rather than assume they are always exactly at the current cargo location. Finally, though we focused on the same kind of linear spring model for the motor-cargo tether as was adopted in the model of [31], our mathematical framework can handle nonlinear tether models (Appendix B). This is important for comparison with experiment, as we spell out below.

With regard to the mathematical analysis of the models, our coarse-grained velocities, diffusivities, and detachment rates within each attachment state reported in Section 4 involve more complex formulas as we have attempted to explicitly model force dependence of the dynamics. This accounting for the effects of the spatial distribution of the motors also is shown in Subsection 4.3.1 to lead to jump contributions of the effective cargo position, with generically nonzero means, when motors attach and detach and the cargo adjusts to the new statistical quasi-equilibrium. Effective velocity is computed in [31] through renewal-reward asymptotics applied to a long time over which the cargo is allowed to go through periods of having no motors attached to the microtubule; the results can be renormalized in the usual way to estimate the average velocity while attached. We have eschewed this setup of allowing reattachment from a completely detached state because it does not allow for a computation of effective diffusivity during a run in which the cargo is attached to a microtubule in the same way it does for effective velocity. Rather we contemplated two asymptotic idealizations of experiments or simulations which terminate when the cargo disassociates from a microtubule: a large ensemble of runs, or a collection of runs which are censored to be sufficiently long. Either setup permits the computation of effective velocity and effective diffusivity through a law of large numbers, based on the random increments of time and cargo displacement during a regeneration cycle of detachment and reattachment to the fully attached state, terminated by a cycle of complete detachment. The effective velocity and diffusivity differ somewhat when computed under the two setups, primarily because the terminal cycle of complete detachment is treated as negligible when only long runs are considered. For homogenous ensembles, as shown in Corollary 1, the effective velocities are in fact identical and the effective diffusivities rigorously close. For kinesin-1/kinesin-2 ensembles, the predictions of effective velocity and effective diffusivity are found in Tables 3 and 4 to differ under the two scenarios by only a few percent in almost all cases.

7.2 Conceptual Findings from Mathematical Results

Inspection of the effective transport formulas presented in Sections 4 and 5 shows (once redimensionalized) that they do not depend on the friction coefficients γ and $\gamma_m^{(i)}$ for the cargo and detached motor dynamics, respectively. These coefficients only need to be small enough that the cargo and detached motor dynamics are indeed fast relative to the attached motor dynamics so that our separation of scales arguments are valid; then their precise values are not relevant. On the other hand, the properties of the motor velocities and diffusivities while attached play clear roles in the determination of associated statistics for two motor systems. The tether spring constant $\kappa^{(i)}$ plays an important role in setting the

force scale of thermal fluctuations $\sqrt{k_B T \boldsymbol{\kappa}^{(i)}}$, whose ratio to stall force (in the nondimensional parameter $s^{(i)}$) and to detachment force scale (in the nondimensional parameter $u^{(i)}$) potentially significantly affect the effective velocities and diffusivities within states (Subsection 4.2), as well as the effective detachment rates (Subsection 4.3.1). Moreover the magnitude of the jumps of the cargo tracking variable at detachment (Subsection 4.3.2) and attachment events (Subsubsection 4.3.3) is also sensitive to the value of the tether spring constant.

These jumps, which perhaps can be associated to cargo flyback [91,50,14], can have a nontrivial impact on the effective transport of ensembles of motors. The mean cargo jump at detachment of a motor is typically nonzero (Eq. (90)), due to relaxation of the cargo to a new equilibrium balancing the applied trap force with one tether rather than two, and the preferential detachment of the leading or trailing motor. But, at least in our model, the cargo jump has mean zero upon reattachment of the second motor (Eqs. (88) and (89)). So in principle, the motor-cargo complex can have a substantial contribution to its effective velocity from a ratcheting process in which, from the state of two attached motors, one detaches, allowing the cargo to rapidly adjust by thermal diffusion to a statistical equilibrium with the attached motor while the detached motor even more quickly equilibrates about the cargo, then the detached motor reattaches to a relaxed configuration (with no net mean cargo position change), and the two attached motors move again toward a more strained configuration leading to motor detachment. This phenomenon caused a speedup in our model of the motor-cargo complex under an assisting trap force which in some cases exceeded the maximum single motor velocity.

We plan to examine this flyback effect with more biophysical detail in future work.

7.3 Future Work for Improved Biophysical Fidelity

Our primary goal in this work has been to set out a mathematical framework for relating the various physicochemical properties of dissimilar cooperative motors on their effective transport as a team. While we have endeavored to parameterize our models for kinesin-1 and kinesin-2 with experimentally-based values, we must note a few issues in this parameterization that require further study before we can meaningfully confront our model predictions to experimental data on multiple motor transport. First of all, our parameters from Table 1 are all from in vitro measurements. As noted as well in McKinley, Athreya, et al [34], the viscosity in cell is substantially higher than water, and this can make the scale separation assumption between cargo and attached motor dynamics (small $\varepsilon^{(i)}$ in Table 2) less tenable. Other biophysical parameters may also have different values in cell [6], though these are even more difficult to establish than their in vitro counterparts. Thus, our focus remains for now on targeting our mathematical framework toward understanding and interpreting in vitro observations.

At least two parameterization problems require substantial development before this can be credibly attempted, though. First of all, to keep focus on the various coarse-graining relationships we employed, we adopted in the main text and in the simulations a simple Hookean spring model for the motor-cargo tether, with a spring constant obtained from

experimental observations of motor-cargo systems with the tether pulled to its natural extension, This linear spring approximation is reasonable for describing small fluctuations of the extended tether, but does not at all model the tether well when its end-to-end separation is smaller than its natural extension. A simple general model used in biophysical simulations of kinesin is to have a linear restoring force under extension from a rest length (varying from 40 nm in [56] to 80 nm in [25] to 110 nm in [22,68]), but no resistance to compression; more complex nonlinear models for extension have also been considered [59,40,92]. Using a fully Hookean model with zero rest length and the experimentally measured linear spring constant (shown in Table 1) leads to an absurd conclusion that the root-mean-square extension of the tether for kinesin-1 is about 5 nm, when of course it should be more like 70 nm. The 5 nm is really an estimate for the magnitude of the fluctuations about this rest length when force on the tether pulls it approximately taut. During a given phase of attachment, this neglect of the rest length of the motor-cargo tether does not necessarily have a strong impact on the calculations – we can imagine the cargo is in fact just approximately this rest length behind the nominal cargo position $Z(t)$ and the motors would feel generally comparable forces as in the simple Hookean model with zero rest length which we used. The big difference, though, would be on the dynamics of the detached motors, which should be fluctuating over a distance comparable to the motor-cargo tether rest length rather than the nominal root-mean-square extension of the Hookean spring model with zero rest length. This would have a big impact on where the detached motors reattach on the microtubule. Thus, the Hookean spring model with zero rest length for the motor-cargo tether cannot be expected to give useful predictions for the transport of actual molecular motors; we must at least extend it to a nonlinear model with no resistance to compression below a finite rest length as in [25,54,67,56,68,32]. In Appendix A, we indicate how nonlinear spring models for the motor-cargo tether can be handled by our mathematical framework – the main complication is the jumps of the cargo tracking variable in Section 4.3 become non-Gaussian. We have here stayed with the purely linear spring model in the main text to minimize technical complications and more clearly illustrate the key concepts in the mathematical coarse-graining of the dynamics of a system of cooperative dissimilar motors. In future work, we will adapt this framework to more biophysically accurate nonlinear spring models for the motor-cargo tether, and examine through this lens various hypotheses and experimental observations regarding the dynamics of cooperative molecular motors.

A second parameterization problem is that of the double exponential force-detachment rate relation (8). Our model is based on a relation between detachment rate and instantaneous force, while what is measured [16,17,70] is the relation between run length and applied trap force. We convert the run length to a detachment rate by dividing by the unloaded velocity, which is a bit crude but arguably a reasonable rough approximation, but the more serious concern is equating the dependence on applied trap force with the dependence on instantanexous force felt by the motor via its tether to the cargo. This leads to particular peculiarities, noted in Section 6, in the absence of trap force, since the force-detachment rate model is discontinuous at zero force. So, in our model, the motor at zero trap force is fluctuating between high detachment rates when the cargo is pulling the motor forward and low detachment rates when the cargo is pulling the motor backward, leading to an inappropriately augmented detachment rate. Rectifying this detachment rate model requires,

in future work, a better statistical inference approach for a relation between instantaneous force and detachment rate that would replicate, under our model, the relation between run length and applied trap force reported in [16,17]. A further potential improvement would be to incorporate the findings of a recent study [70] suggesting a different structure for the dependence of the detachment rate against a truly longitudinal applied force on kinesin-1.

7.4 Future Mathematical Directions

A mathematical question for future work is to examine whether the coarse-grained model developed here would change if we started with a discrete stepping model [26,35-37,5,38,39,30,25] for the motor dynamics, rather than the coarse-grained stochastic differential equation model (1) used here. This is essentially a question of how the coarse-graining of a jump process model for the motor dynamics into a stochastic differential equation interacts with the coarse-graining procedures developed here. Perhaps the cargo fluctuations interacting with the discrete stepping model would give rise to a different effective dynamics (20) for the attached motors.

Another question is how our detailed analysis of effective transport of an ensemble of two cooperative motors can be extended to more general scenarios of multiple motors attached to a cargo. The initial coarse-graining steps over the detached motor and cargo dynamics in Section 3 applied to an arbitrary number N of cooperative motors, only at the cost of complexity, but the coarse-graining over the attached motor dynamics in Section 4 relied on the ability to homogenize the attached motor dynamics for the case $N = 2$ via the explicit stationary distribution for an autonomous single-variable SDE for the separation R between the motors. For $N > 2$, we would have $N - 1$ coupled degrees of freedom for the internal configuration of the motors, whose stationary distribution does not seem possible to compute analytically due to the absence of a potential structure for the drift. The work of Miles, Lawley, and Keener [31] could readily handle arbitrary numbers of cooperative motors because their model did not include explicit reference to the spatial configuration of the motors.

A complementary extension to the tug-of-war case of two opposing motors is problematic because the scale separation assumption between attached motor dynamics and the detachment process is unlikely to be supported under realistic models for the detachment rate. For two cooperative motors, the separation between them can plausibly be thought to reach a stationary distribution before they detach, and the nondimensional analysis in Section 3 provides some quantitative support. Recall that the predictions from the asymptotic theory were not so accurate under the double exponential detachment rate model for a kinesin-2/kinesin-2 ensemble (Table 4) under hindering trap force because the detachment may actually be governed by when a fluctuation, perhaps from the initial reattachment configuration, in the separation of the motors caused the leading motor to feel a higher force and an exponentially increased detachment rate. This phenomenon would be manifest more generally in the case of opposing motors because their separation would directly increase by their dynamics, only stabilized when the forces on the motors are substantial enough to slow their rate of separation, but then the detachment rate would also be substantially increased. Only if the stall force for the motors were considerably less than

the force scale of detachment could the dynamics of a pair of attached motors plausibly reach a stationary distribution before detachment. But this is certainly not true for kinesin-1 or kinesin-2 (Table 1)) and does not appear relevant for biological motors in general [93]. A fundamentally different mathematical analysis would be required to characterize the statistics of displacement and detachment from a state of two attached opposing motors when the dependence of the detachment rate on force varies strongly over the scale of the stall force of the motors.

While the model and analysis here considered the case of the cooperative motors all being associated with a single microtubule, the model and calculations could still be appropriate for the context of the motors attaching and detaching from a parallel bundle of microtubules, so long as their spacing is tight enough that the transverse displacements of the motors could be treated as having a negligible effect on the dynamics along the longitudinal direction, and the cargo dynamics are not much affected by steric interaction with the microtubule bundles. These conditions are probably not satisfied in most biologically relevant contexts, though they could apply to certain engineered in vitro configurations. But once the microtubule network is not aligned with a common polarity, the motor dynamics will be affected by tug-of-war considerations and the coarse-graining of attached motor dynamics would require a different approach, as for the case of opposing motors.

Availability of data and material (data transparency)

Simulation data was generated to test the model. As the main product of this manuscript is the theoretical framework, we do not view the simulated data as being of sufficient value to make publicly available.

Acknowledgements

This work grew out of conversations between JF and PRK while both were long term visitors at the Isaac Newton Institute for the program on “Stochastic Dynamics in Biology: Numerical Methods and Applications.” The authors also would like to thank Will Hancock for discussions informing the model development. PRK would also like to acknowledge early discussions with Leonid Bogachev, Leonid Koralov, and Yuri Makhnovskii which helped me map out the general mathematical framework and approaches, while we were all supported as long-term visitors at the Zentrum für Interdisziplinäre Forschung for the program on “Stochastic Dynamics: Mathematical Theory and Applications.” Here we’ve managed to work out one ofthe easier cases we considered…

Funding

The work of JF and PRK are partially supported by National Institutes of Health grant R01GM122082 and PRK was partially supported by a grant from the Simons foundation. The work of JK is partially supported by an National Science Foundation RTG grant 1344962.

A Appendix: A note on nonlinear spring models

A linear model for representing the tether between the motor and the cargo is not particularly accurate. Better theoretical tether models can involve a model which is Hookean for extension beyond a rest length, but offers no resistance to compression [25,54,67,56,68,32], a sigmoidal stiffness dependence on force [59], or a multiple-component model for the motor-cargo tether including separate models for the neck linker and stalk [40]. We may generalize the averaging results by considering a nonlinear spring

$$F^{(i)}(r) = \bar{F}^{(i)}\Phi'^{(i)}(r \,/\, L_c^{(i)}) \;\; 1 \le i \le N\,. \tag{94}$$

Here $\Phi^{(i)}(r)$ is a nondimensionalized spring potential, $L_c^{(i)}$ is an appropriate length scale, and $\bar{F}^{(i)}$ is a characteristic force magnitude for each motor index i. We define $\kappa^{(i)} \equiv \bar{F}^{(i)} \,/\, L_c^{(i)}$ as an "effective" spring constant of the nonlinear spring; it agrees with the usual spring constant when the spring force model is purely Hookean, as in the main text.

With the same nondimensionalization as before, the equations of motion become, for $1 \le i \le N$,

$$\begin{aligned} &d\widetilde{X}^{(i)}(\widetilde{t}) = \\ &\left(\varepsilon^{(i)} g(s^{(i)}\widetilde{\kappa}^{(i)}(\lambda^{(i)})^{-1}\Phi'^{(i)}(\lambda^{(i)}(\widetilde{X}^{(i)}(\widetilde{t}) - \widetilde{Z}(\widetilde{t})))d\widetilde{t} + \sqrt{\hat{\rho}^{(i)}\varepsilon^{(i)}}dW^{(i)}(\widetilde{t})\right) \times Q^{(i)}(\widetilde{t}) \\ &+ \left(-\left(\Gamma^{(i)}\lambda^{(i)}\right)^{-1}\widetilde{\kappa}^{(i)}\Phi'^{(i)}\left(\lambda^{(i)}\left(\widetilde{X}^{(i)}\widetilde{t} - \widetilde{Z}(\widetilde{t})\right)\right)d\widetilde{t} + (\Gamma^{(i)})^{-1\,/\,2}dW^{(i)}(\widetilde{t})\right) \\ &\times (1 - Q^{(i)}(\widetilde{t})), \end{aligned} \tag{95}$$

$$d\widetilde{Z}(\widetilde{t}) = \left(\sum_{j=1}^{N} (\lambda^{(i)})^{-1}\widetilde{\kappa}^{(i)}\Phi'(\lambda^{(i)}(\widetilde{X}^{(j)}(\widetilde{t}) - \widetilde{Z}(\widetilde{t}))) - \widetilde{F}_T\right)d\widetilde{t} + dW_z(\widetilde{t}), \tag{96}$$

where we have introduced the new nondimensional parameter

$$\lambda^{(i)} = \frac{\sqrt{2k_BT \,/\, \bar{\kappa}}}{L_c^{(i)}}\,. \tag{97}$$

which describes the length-scale of thermally induced variations on the tether relative to the length scale of variation of the tether force law. Calculations for the averaged drifts $\vec{g}^{(i)}$, and thus G_+ and G_-, are similar, but now involve pairing drift functions with non-Gaussian stationary distributions for unattached motors and cargo (the forms for these equations are nearly identical to those found in Appendix A in McKinley, Athreya, et al [34]). For detachment jumps, no assumptions of distribution type are made for $p_R(r)$, and therefore the calculations for distributions in Subsection 4.3.2 only need to be adjusted to refer to the mean cargo position under nonlinear tethers.

The random variable $\Delta M_i^{(a)}$ describing the change of position of the cargo tracking variable after motor attachment may be computed similarly as in Subsection 4.3.3, but it will no longer be normally distributed or have mean zero in general. The calculations in Section 5 otherwise go through for a nonlinear tether model, with only the modified contribution to the moments of the cargo tracking variable changes at attachment and detachment jumps.

B Appendix: Derivation of effective diffusion for two motors

The following derivation for the effective diffusion of the cargo tracking variable during a state with both motors attached to the microtubule follows the multiscale expansion method

illustrated in Pavliotis and Stuart [75], with rigorous exposition in Veretennikov and Pardoux [94] for the unbounded state space case relevant to our application. Having computed the effective drift $V_{1,2}$ in Eq. (33) in this state, we pass to a diffusive scaling centered about this mean drift $\bar{t} \to t / \varepsilon^2$, $M \to \varepsilon(M - V_{1,2}t)$, with the internal configuration variable R unscaled ($R \to R$). Note in this appendix, ε is just a formal small parameter used to push to long time; it is unrelated to the physically meaningful nondimensional parameters $\varepsilon^{(i)}$ and $\bar{\varepsilon}$ in the main text. Moreover, for simplicity for calculations within this appendix, we use the undecorated variables t,M,R to describe the dynamics under this centered diffusive rescaling, which read:

$$dM(t) = \frac{1}{\varepsilon}(G_+(R(t)) - V_{1,2})dt + \frac{\sqrt{\rho^{(1)}(\tilde{\kappa}^{(1)})^2}}{2}dW^{(1)}(t) + \frac{\sqrt{\rho^{(2)}(\tilde{\kappa}^{(2)})^2}}{2}dW^{(2)}t \tag{98}$$

$$dR(t) = \frac{1}{\varepsilon^2}G_-(R(t))dt + \frac{1}{\varepsilon}\left(\sqrt{\rho^{(1)}}dW^{(1)}(t) - \sqrt{\rho^{(2)}}dW^{(2)}(t)\right). \tag{99}$$

The infinitesimal generator $\mathscr{L}$ for (99)-(100) is defined by its action on a test function $v = v(m,r)$, with

$$\mathscr{L}v(m,r) = \mathbf{h} \cdot \nabla v + \frac{1}{2}\Gamma : \nabla\nabla v\,. \tag{100}$$

Here $\mathbf{h}(m,r) = ((G_+(r) - V_{1,2})/\varepsilon, G_-(r)/\varepsilon^2)$ is the drift vector, and $\frac{1}{2}\Gamma$ is the diffusion tensor, where

$$\begin{aligned}\Gamma &= \begin{bmatrix} \frac{\sqrt{\rho^{(1)}(\tilde{\kappa}^{(1)})^2}}{2} & \frac{\sqrt{\rho^{(2)}(\tilde{\kappa}^{(2)})^2}}{2} \\ \frac{\sqrt{\rho^{(1)}}}{\varepsilon} & -\frac{\sqrt{\rho^{(2)}}}{\varepsilon} \end{bmatrix} \begin{bmatrix} \frac{\sqrt{\rho^{(1)}(\tilde{\kappa}^{(1)})^2}}{2} & \frac{\sqrt{\rho^{(2)}(\tilde{\kappa}^{(2)})^2}}{2} \\ \frac{\sqrt{\rho^{(1)}}}{\varepsilon} & -\frac{\sqrt{\rho^{(2)}}}{\varepsilon} \end{bmatrix}^T \\ &= \begin{bmatrix} \frac{\rho^{(1)}(\tilde{\kappa}^{(1)})^2 + \rho^{(2)}(\tilde{\kappa}^{(2)})^2}{4} & \frac{\rho^{(1)}\tilde{\kappa}^{(1)} - \rho^{(2)}\tilde{\kappa}^{(2)}}{2\varepsilon} \\ \frac{\rho^{(1)}\tilde{\kappa}^{(1)} - \rho^{(2)}\tilde{\kappa}^{(2)}}{2\varepsilon} & \frac{\rho^{(1)} + \rho^{(2)}}{\varepsilon^2} \end{bmatrix}. \end{aligned} \tag{101}$$

We have also used notation for the Frobenius inner product for matrices, where for matrices $A = (a_{i,j})_{nxm}$ and $B = (b_{i,j})_{nxm}$, we define $A : B = \Sigma_{i,j}a_{i,j}b_{i,j}$.

We may write out (101) explicitly as

$$\begin{aligned}\mathscr{L}v(m,r) &= \mathbf{h}\cdot\nabla v + \frac{1}{2}\Gamma:\nabla\nabla v\\ &= \frac{1}{\boldsymbol{\varepsilon}}(G_+(r)-V_{1,2})v_m + \frac{1}{\boldsymbol{\varepsilon}^2}G_-(r)v_r\\ &+ \frac{1}{2}\left[\left(\frac{\boldsymbol{\rho}^{(1)}(\widetilde{\boldsymbol{\kappa}}^{(1)})^2+\boldsymbol{\rho}^{(2)}(\widetilde{\boldsymbol{\kappa}}^{(2)})^2}{4}\right)v_{mm} + \frac{\boldsymbol{\rho}^{(1)}\widetilde{\boldsymbol{\kappa}}^{(1)}-\boldsymbol{\rho}^{(2)}\widetilde{\boldsymbol{\kappa}}^{(2)}}{\boldsymbol{\varepsilon}}v_{mr} + \left(\frac{\boldsymbol{\rho}^{(1)}+\boldsymbol{\rho}^{(2)}}{\boldsymbol{\varepsilon}^2}\right)v_{rr}\right].\end{aligned} \tag{102}$$

The generator may be decomposed to match powers of ε as

$$\mathscr{L} = \frac{1}{\boldsymbol{\varepsilon}^2}\mathscr{L}_0 + \frac{1}{\boldsymbol{\varepsilon}}\mathscr{L}_1 + \mathscr{L}_2, \tag{103}$$

with

$$\mathscr{L}_0 = G_-(r)\,\partial_r + \frac{\boldsymbol{\rho}^{(1)}+\boldsymbol{\rho}^{(2)}}{2}\partial_{rr}, \tag{104}$$

$$\mathscr{L}_1 = \frac{\boldsymbol{\rho}^{(1)}\widetilde{\boldsymbol{\kappa}}^{(1)}-\boldsymbol{\rho}^{(2)}\widetilde{\boldsymbol{\kappa}}^{(2)}}{2}\partial_{mr} + (G_+(r)-V_{1,2})\,\partial_m, \tag{105}$$

$$\mathscr{L}_2 = \left(\frac{\boldsymbol{\rho}^{(1)}(\widetilde{\boldsymbol{\kappa}}^{(1)})^2+\boldsymbol{\rho}^{(2)}(\widetilde{\boldsymbol{\kappa}}^{(2)})^2}{8}\right)\partial_{mm}\,. \tag{106}$$

Assuming a multiscale solution $v = v_0 + \varepsilon v_1 + \varepsilon^2 v_2 + \ldots$ for the backward Kolmogorov equation

$$\frac{\partial v}{\partial t} = \mathscr{L}_v, \tag{107}$$

we match powers of orders $1/\varepsilon^2$, $1/\varepsilon$, and 1 to obtain

$$\mathscr{L}_0 v_0 = 0, \tag{108}$$

$$-\mathscr{L}_0 v_1 = \mathscr{L}_1 v_0, \tag{109}$$

$$-\mathscr{L}_0 v_2 = -\frac{\partial v_0}{\partial t} + \mathscr{L}_1 v_1 + \mathscr{L}_2 v_0\,. \tag{110}$$

The first equation implies that v_0 is only a function of m and t. From here, the second equation may be simplified to

$$-\mathscr{L}_0 v_1 = (G_+(r)-V_{1,2})\,\partial_m v_0(m,t)\,. \tag{111}$$

As the operator $\mathscr{L}_0$ only depends on r, we may express v_1 as

$$v_1(m,r,t) = \chi(r)\,\partial_m v_0(m,t)\,. \tag{112}$$

Proceeding to the third equation of the asymptotic expansion, the Fredholm alternative states that for (111) to have a solution, its right hand side must be orthogonal to $p_R(r)$, or

$$\begin{aligned}\frac{\partial v_0}{\partial t} &= \int_{\mathbb{R}} p_R(r)\mathscr{L}_2 v_0(m,t)dt + \int_{\mathbb{R}} p_R(r)\mathscr{L}_1(\chi(r)\,\partial_m v_0(m,t))dr \\ &:= I_1 + I_2\,.\end{aligned} \tag{113}$$

We look at each integral in turn. First,

$$\begin{aligned}I_1 &= \int_{\mathbb{R}} p_R(r)\mathscr{L}_2 v_0(m,t)dr \\ &= \int_{\mathbb{R}} p_R(r)\left[(G_+(r) - V_{1,2})\,\partial_m v_0(m,t) + \left(\frac{\boldsymbol{\rho}^{(1)}(\widetilde{\boldsymbol{\kappa}}^{(1)})^2 + \boldsymbol{\rho}^{(2)}(\widetilde{\boldsymbol{\kappa}}^{(2)})^2}{8}\right)\partial_{mm} v_0(m,t)\right]dr \\ &= \left(\frac{\boldsymbol{\rho}^{(1)}(\widetilde{\boldsymbol{\kappa}}^{(1)})^2 + \boldsymbol{\rho}^{(2)}(\widetilde{\boldsymbol{\kappa}}^{(2)})^2}{8}\right)\partial_{mm} v_0(m,t)\end{aligned} \tag{114}$$

.

The second integral may be broken up further, as

$$\begin{aligned}I_2 &= \int_{\mathbb{R}} p_R(r)\mathscr{L}_1(\chi(r)\,\partial_m v_0(m,t))dr \\ &= \int_{\mathbb{R}} p_R(r)\left[\left(\frac{\boldsymbol{\rho}^{(1)}\boldsymbol{\kappa}^{(1)} - \boldsymbol{\rho}^{(2)}\boldsymbol{\kappa}^{(2)}}{2}\right)\partial_{mr}(\chi(r)\,\partial_m v_0(m,t))\right. \\ &\quad \left. +\ (G_+(r) - V_{1,2})\,\partial_m(\chi(r)\,\partial_m v_0(m,t))\right]dr \\ &:= I_3 + I_4\,.\end{aligned} \tag{115}$$

The first part satisfies

$$\begin{aligned}I_3 &= \int_{\mathbb{R}} p_R(r)\left(\frac{\boldsymbol{\rho}^{(1)}\widetilde{\boldsymbol{\kappa}}^{(1)} - \boldsymbol{\rho}^{(2)}\widetilde{\boldsymbol{\kappa}}^{(2)}}{2}\right)\partial_{mr}(\chi(r)\,\partial_m v_0(m,t))dr \\ &= \left(\left(\frac{\boldsymbol{\rho}^{(1)}\widetilde{\boldsymbol{\kappa}}^{(1)} - \boldsymbol{\rho}^{(2)}\widetilde{\boldsymbol{\kappa}}^{(2)}}{2}\right)\int_{\mathbb{R}} p_R(r)\,\partial_r\chi(r)dr\right)\partial_{mm} v_0(m,t) \\ &:= A_1\,\partial_{mm} v_0(m,t)\,.\end{aligned} \tag{116}$$

Finally, we have

$$\begin{aligned} I_4 &= \int_{\mathbb{R}} p_R(r)[(G_+(r) - V_{1,2})\,\partial_m(\chi(r)\,\partial_m v_0(m,t))]dr \\ &= \int_{\mathbb{R}} p_R(r)[(G_+(r) - V_{1,2})\chi(r)]dr\,\partial_{mm} v_0(m,t) \\ &\coloneqq A_2\,\partial_{mm} v_0(m,t)\,. \end{aligned} \tag{117}$$

The closed form equation for $v_0(m,t)$ is thus given by

$$\frac{\partial v_0}{\partial t} = \frac{1}{2}\left(\frac{\boldsymbol{\rho}^{(1)}(\widetilde{\boldsymbol{\kappa}}^{(1)})^2 + \boldsymbol{\rho}^{(2)}(\widetilde{\boldsymbol{\kappa}}^{(2)})^2}{4} + 2A_1 + 2A_2\right)\partial_{mm} v_0(m,t), \tag{118}$$

and is the backward Kolmogorov equation for the SDE

$$\begin{aligned} dM(t) &= \sqrt{\frac{\boldsymbol{\rho}^{(1)}(\widetilde{\boldsymbol{\kappa}}^{(1)})^2 + \boldsymbol{\rho}^{(2)}(\widetilde{\boldsymbol{\kappa}}^{(2)})^2}{4} + 2A_1 + 2A_2}\,dW(t) \\ &\equiv \sqrt{2D^{(1,2)}}\,dW(t), \end{aligned} \tag{119}$$

where $W(t)$ is a standard Brownian motion.

Now we compute explicit expressions for constants A_1 and A_2. This involves solving the cell problem for χ, given by

$$\begin{aligned} -G_-(r)\chi'(r) - \left(\frac{\boldsymbol{\rho}^{(1)} + \boldsymbol{\rho}^{(2)}}{2}\right)\chi''(r) &= \widetilde{g}_+(r), \\ \int_{\mathbb{R}} \chi(r)\,p_R(r)dr &= 0, \end{aligned} \tag{120}$$

where we define $\widetilde{g}_+(r) = G_+(r) - V_{1,2}$. If we rewrite (121), using an integration factor $\mu(r)$, as

$$[\boldsymbol{\mu}(r)\chi'(r)]' = -\boldsymbol{\mu}(r)\widetilde{g}_+(r)\left(\frac{2}{\boldsymbol{\rho}^{(1)} + \boldsymbol{\rho}^{(2)}}\right), \tag{121}$$

then it is straightforward to show that $\mu(r)$ is in fact equal to the stationary distribution $p_R(r)$. Integrating out (122) leaves us with

$$\chi'(r) = -\int_{-\infty}^{r} \widetilde{g}_+(r')\left(\frac{2}{\boldsymbol{\rho}^{(1)} + \boldsymbol{\rho}^{(2)}}\right)p_R(r')dr' \;/\; p_R(r) + C \;/\; p_R(r) \tag{122}$$

for some unknown integration constant C. By the subexponential growth requirement on χ and χ' [94], it follows that $C = 0$. From (117),

$$\begin{aligned} A_1 &= \left(\frac{\boldsymbol{\rho}^{(2)}\widetilde{\boldsymbol{\kappa}}^{(2)} - \boldsymbol{\rho}^{(1)}\widetilde{\boldsymbol{\kappa}}^{(1)}}{\boldsymbol{\rho}^{(1)} + \boldsymbol{\rho}^{(2)}}\right)\int_{\mathbb{R}}\int_{-\infty}^{r} \widetilde{g}_+(r')p_R(r')dr'dr \\ &= \left(\frac{\boldsymbol{\rho}^{(1)}\widetilde{\boldsymbol{\kappa}}^{(1)} - \boldsymbol{\rho}^{(2)}\widetilde{\boldsymbol{\kappa}}^{(2)}}{\boldsymbol{\rho}^{(1)} + \boldsymbol{\rho}^{(2)}}\right)\int_{\mathbb{R}} \widetilde{g}_+(r)p_R(r)\cdot r dr\,. \end{aligned} \tag{123}$$

The last equality used integration by parts, in which the boundary term vanishes under the assumption that $p_R(r) = o(1/r^2)$ as $r \to \pm\infty$. The calculation for A_2 (118) follows from integration by parts, with

$$\begin{aligned} A_2 &= \int_{-\infty}^{\infty} \chi(r)\widetilde{g}_+(r)p_R(r)dr = -\int_{-\infty}^{\infty} \chi(r)(\mathscr{L}_0\chi(r))p_R(r)dr \\ &= -\int_{-\infty}^{\infty} \chi(r)\left(G_-(r)\chi'(r) + \left(\frac{\boldsymbol{\rho}^{(1)}+\boldsymbol{\rho}^{(2)}}{2}\right)\chi''(r)\right)p_R(r)dr \\ &= \int_{-\infty}^{\infty}\left(\frac{\boldsymbol{\rho}^{(1)}+\boldsymbol{\rho}^{(2)}}{2}\right)\chi'(r)^2 p_R(r)dr \\ &= \int_{-\infty}^{\infty}\left(\frac{2}{\boldsymbol{\rho}^{(1)}+\boldsymbol{\rho}^{(2)}}\right)\left(\int_{-\infty}^{r}\widetilde{g}_+(r')p_R(r')dr'\right)^2\frac{1}{p_R(r)}dr\,. \end{aligned} \tag{124}$$

References

1. Alberts B, Molecular Biology of the Cell (CRC Press, 2017). URL https://books.google.com/books?id=2xIwDwAAQBAJ
2. Phillips R, Kondev J, Theriot J, Garcia H, Physical biology of the cell (Garland Science, 2012)
3. Hancock WO, Howard J, Molecular motors pp. 243–269 (2003)
4. Hancock WO, Nature reviews Molecular cell biology 15(9), 615 (2014) [PubMed: 25118718]
5. Wang Z, Li M, Phys. Rev. E 80(4), 041923 (2009). DOI 10.1103/PhysRevE.80.041923
6. Kunwar A, Tripathy SK, Xu J, Mattson MK, Anand P, Sigua R, Vershinin M, McKenney RJ, Clare CY, Mogilner A, et al., Proceedings of the National Academy of Sciences 108(47), 18960 (2011)
7. Müller MJ, Klumpp S, Lipowsky R, Proceedings of the National Academy of Sciences 105(12), 4609 (2008)
8. Mallik R, Rai AK, Barak P, Rai A, Kunwar A, Trends in cell biology 23(11), 575 (2013) [PubMed: 23877011]
9. Lombardo AT, Nelson SR, Ali MY, Kennedy GG, Trybus KM, Walcott S, Warshaw DM, Nature communications 8, 15692 (2017)
10. Rai AK, Rai A, Ramaiya AJ, Jha R, Mallik R, Cell 152(1-2), 172 (2013) [PubMed: 23332753]
11. Smith JD, McKinley SA, Bulletin of Mathematical Biology 80(8), 2088 (2018). DOI 10.1007/s11538-018-0448-9. URL 10.1007/s11538-018-0448-9 [PubMed: 29869045]
12. Müller MJ, Klumpp S, Lipowsky R, Journal of Statistical Physics 133(6), 1059 (2008)
13. Klumpp S, Lipowsky R, Proceedings of the National Academy of Sciences of the United States of America 102(48), 17284 (2005) [PubMed: 16287974]
14. Feng Q, Mickolajczyk KJ, Chen GY, Hancock WO, Biophysical journal 114(2), 400 (2018) [PubMed: 29401437]
15. Spudich JA, Rice SE, Rock RS, Purcell TJ, Warrick HM, Cold Spring Harbor Protocols 2011(11), pdb (2011)
16. Milic B, Andreasson JO, Hancock WO, Block SM, Proceedings of the National Academy of Sciences 111(39), 14136 (2014)
17. Milic B, Andreasson JO, Hogan DW, Block SM, Proceedings of the National Academy of Sciences 114(33), E6830 (2017)
18. Andreasson JO, Shastry S, Hancock WO, Block SM, Current Biology 25(9), 1166 (2015) [PubMed: 25866395]
19. Leduc C, Campàs O, Zeldovich KB, Roux A, Jolimaitre P, Bourel-Bonnet L, Goud B, Joanny JF, Bassereau P, Prost J, Proceedings of the National Academy of Sciences of the United States of America 101(49), 17096 (2004) [PubMed: 15569933]
20. Block SM, Goldstein LS, Schnapp BJ, Nature 348(6299), 348 (1990) [PubMed: 2174512]

21. Vale RD, Funatsu T, Pierce DW, Romberg L, Harada Y, Yanagida T, Nature 380(6573), 451 (1996) [PubMed: 8602245]
22. Kunwar A, Mogilner A, Physical biology 7(1), 016012 (2010)
23. Lipowsky R, Beeg J, Dimova R, Klumpp S, Liepelt S, MüLler MJI, Valleriani A, Biophysical Reviews and Letters 04(01n02), 77 (2009). DOI 10.1142/S1793048009000946. URL 10.1142/S1793048009000946
24. Klumpp S, Keller C, Berger F, Lipowsky R, in Multiscale Modeling in Biomechanics and Mechanobiology, ed. by De S, Hwang W, Kuhl E (Springer London, 2015), pp. 27–61
25. Keller C, Berger F, Liepelt S, Lipowsky R, Journal of Statistical Physics 150(2), 205 (2013). DOI 10.1007/s10955-012-0662-z. URL 10.1007/s10955-012-0662-z
26. Bouzat S, Physical Review E 93(1), 012401 (2016) [PubMed: 26871095]
27. Jamison DK, Driver JW, Rogers AR, Constantinou PE, Diehl MR, Biophysical Journal 99(9), 2967 (2010). DOI doi: 10.1016/j.bpj.2010.08.025. URL http://www.sciencedirect.com/science/article/pii/S000634951000994X [PubMed: 21044594]
28. McLaughlin RT, Diehl MR, Kolomeisky AB, Soft Matter 12(1), 14 (2015). DOI 10.1039/C5SM01609F. URL http://pubs.rsc.org/en/content/articlelanding/2016/sm/c5sm01609f
29. Srinivas B, Gopalakrishnan M, Physical Biology 16(1), 016006 (2018). DOI 10.1088/1478-3975/aaefa6. URL 10.1088/F1478-3975/Faaefa6 [PubMed: 30524046]
30. Driver JW, Rogers AR, Jamison DK, Das RK, Kolomeisky AB, Diehl MR, Phys. Chem. Chem. Phys 12(35), 10398 (2010). URL 10.1039/C0CP00117A [PubMed: 20582368]
31. Miles C, Lawley S, Keener J, SIAM Journal on Applied Mathematics 78(5), 2511 (2018). DOI 10.1137/17M1156824. URL 10.1137/17M1156824
32. Furuta K, Furuta A, Toyoshima YY, Amino M, Oiwa K, Kojima H, Proceedings of the National Academy of Sciences 110(2), 501 (2013)
33. Encalada SE, Szpankowski L, Xia C.h., Goldstein LS, Cell 144(4), 551 (2011). DOI 10.1016/j.cell.2011.01.021. URL http://linkinghub.elsevier.com/retrieve/pii/S0092867411000602 [PubMed: 21335237]
34. McKinley SA, Athreya A, Fricks J, Kramer PR, Journal of theoretical biology 305, 54 (2012) [PubMed: 22575549]
35. DeVille REL, Vanden-Eijnden E, Biophysical Journal 95, 2681 (2008) [PubMed: 18556760]
36. DeVille REL, Vanden-Eijnden E, Bull. Math. Biol 70(2), 484 (2008) [PubMed: 17973174]
37. Hughes J, Hancock WO, Fricks J, Bulletin of mathematical biology 74(5), 1066 (2012) [PubMed: 21997362]
38. Elston TC, Journal of Mathematical Biology 41, 189 (2000) [PubMed: 11072755]
39. Kolomeisky AB, Fisher ME, Annual Review of Physical Chemistry 58(1), 675 (2007). DOI 10.1146/annurev.physchem.58.032806.104532. URL 10.1146/annurev.physchem.58.032806.104532
40. Hendricks AG, Epureanu BI, Meyhöfer E, Physical Review E 79(3), 031929 (2009). DOI 10.1103/PhysRevE.79.031929. URL 10.1103/PhysRevE.79.031929
41. Mickolajczyk KJ, Hancock WO, Biophysical Journal 112(12), 2615 (2017). DOI 10.1016/j.bpj.2017.05.007. URL http://linkinghub.elsevier.com/retrieve/pii/S0006349517305118 [PubMed: 28636917]
42. Vanvreeswijk C, Abbott LF, SIAM Journal on Applied Mathematics 53(1), 253 (1993). URL http://www.jstor.org/stable/2102284. ArticleType: research-article / Full publication date: Feb., 1993 / Copyright © 1993 Society for Industrial and Applied Mathematics
43. Chariker L, Young LS, Journal of Computational Neuroscience 38(1), 203 (2015). DOI 10.1007/s10827-014-0534-4. URL 10.1007/s10827-014-0534-4 [PubMed: 25326365]
44. Kovačič G, Tao L, Rangan AV, Cai D, Physical Review E (Statistical, Nonlinear, and Soft Matter Physics) 80(2), 021904 (2009). DOI 10.1103/PhysRevE.80.021904. URL http://link.aps.org/abstract/PRE/v80/e021904
45. Hopfield JJ, Herz AV, Proceedings of the National Academy of Sciences of the United States of America 92(15), 6655 (1995). URL http://www.pnas.org/content/92/15/6655.abstract [PubMed: 7624307]

46. Ostojic S, Brunel N, Hakim V, Journal of Computational Neuroscience 26(3), 369 (2009). DOI 10.1007/s10827-008-0117-3. URL 10.1007/s10827-008-0117-3 [PubMed: 19034642]
47. Shkarayev MS, Kovačič G, Cai D, Physical Review E 85(3), 036104 (2012). DOI 10.1103/PhysRevE.85.036104. URL 10.1103/PhysRevE.85.036104
48. Zillmer R, Brunel N, Hansel D, Physical Review E (Statistical, Nonlinear, and Soft Matter Physics) 79(3), 031909 (2009). DOI 10.1103/PhysRevE.79.031909. URL http://link.aps.org/abstract/PRE/v79/e031909
49. Newhall KA, Kovačič G, Kramer PR, Zhou D, Rangan AV, Cai D, Commun. Math. Sci 8(2), 541 (2010). URL http://projecteuclid.org/getRecord?id=euclid.cms/1274816894
50. Sanghavi P, D'Souza A, Rai A, Rai A, Padinhatheeri R, Mallik R, Current Biology 28(9), 1460 (2018). DOI 10.1016/j.cub.2018.03.041. URL https://www.cell.com/current-biology/abstract/S0960-9822(18)30370-1 [PubMed: 29706510]
51. Cox DR, Isham V, Point processes, vol. 12 (CRC Press, 1980)
52. Cox DR, Journal of the Royal Statistical Society: Series B (Methodological) 17(2), 129 (1955)
53. Baker JE, Thomas DD, Biophysical journal 79(4), 1731 (2000) [PubMed: 11023881]
54. Kunwar A, Vershinin M, Xu J, Gross SP, Current biology 18(16), 1173 (2008) [PubMed: 18701289]
55. Bergman JP, Bovyn MJ, Doval FF, Sharma A, Gudheti MV, Gross SP, Allard JF, Vershinin MD, Proceedings of the National Academy of Sciences 115(3), 537 (2018). DOI 10.1073/pnas.1707936115. URL http://www.pnas.org/content/115/3/537
56. Arpăg G, Norris SR, Mousavi SI, Soppina V, Verhey KJ, Hancock WO, Tüzel E, Biophysical Journal 116(6), 1115 (2019). DOI 10.1016/j.bpj.2019.01.036. URL http://www.cell.com/biophysj/abstract/S0006-3495(19)30106-7 [PubMed: 30824116]
57. Materassi D, Salapaka M, Roychowdhury S, Hays T, BMC biophysics 6(1), 14 (2013) [PubMed: 24237658]
58. Talukdar S, Bhaban S, Materassi D, Salapaka M, in Decision and Control (CDC), 2016 IEEE 55th Conference on (IEEE, 2016), pp. 3356–3362
59. Uppulury K, Efremov AK, Driver JW, Jamison DK, Diehl MR, Kolomeisky AB, Cellular and Molecular Bioengineering 6(1), 38 (2013). DOI 10.1007/s12195-012-0260-9. URL 10.1007/s12195-012-0260-9 [PubMed: 24489614]
60. Berger F, Müller MJI, Lipowsky R, EPL (Europhysics Letters) 87(2), 28002 (2009). DOI 10.1209/0295-5075/87/28002. URL http://iopscience.iop.org/0295-5075/87/2/28002
61. Li X, Lipowsky R, Kierfeld J, Biophysical Journal 104(3), 666 (2013). DOI 10.1016/j.bpj.2012.11.3834. URL http://www.sciencedirect.com/science/article/pii/S0006349512051235 [PubMed: 23442917]
62. Peskin CS, Oster G, Biophysical Journal 68, 202s (1995) [PubMed: 7787069]
63. Krishnan A, Epureanu BI, Bulletin of mathematical biology 73(10), 2452 (2011) [PubMed: 21327881]
64. Shtylla B, Keener JP, Physical Review E 91(4), 042711 (2015). DOI 10.1103/PhysRevE.91.042711. URL 10.1103/PhysRevE.91.042711
65. Coppin CM, Pierce DW, Hsu L, Vale RD, Proceedings of the National Academy of Sciences 94(16), 8539 (1997). DOI 10.1073/pnas.94.16.8539. URL https://www.pnas.org/content/94/16/8539
66. Kojima H, Muto E, Higuchi H, Yanagida T, Biophysical Journal 73(4), 2012 (1997) [PubMed: 9336196]
67. Takshak A, Kunwar A, Protein Science 25(5), 1075 (2016). DOI 10.1002/pro.2905. URL 10.1002/pro.2905/abstract [PubMed: 26890030]
68. Erickson RP, Jia Z, Gross SP, Yu CC, PLoS Comput Biol 7(5), e1002032 (2011). DOI 10.1371/journal.pcbi.1002032. URL 10.1371/journal.pcbi.1002032 [PubMed: 21573204]
69. Visscher K, Schnitzer MJ, Block SM, Nature 400(6740), 184 (1999) [PubMed: 10408448]
70. Khataee H, Howard J, Physical Review Letters 122(18), 188101 (2019). DOI 10.1103/PhysRevLett.122.188101. URL 10.1103/PhysRevLett.122.188101 [PubMed: 31144901]
71. Bell GI, et al., Science 200(4342), 618 (1978) [PubMed: 347575]

72. Bressloff PC, Newby JM, Physical Review E 83(6), 061139 (2011)
73. Lin CC, Segel LA, Mathematics applied to deterministic problems in the natural sciences (SIAM, 1988)
74. Novozhilov IV, Fractional analysis: Methods of motion decomposition (Springer Science & Business Media, 2012)
75. Pavliotis G, Stuart A, Multiscale methods: averaging and homogenization (Springer Science & Business Media, 2008)
76. Holmes MH, Introduction to perturbation methods, Texts in Applied Mathematics, vol. 20 (Springer-Verlag, New York, 1995)
77. Skorokhod AV, Hoppensteadt FC, Salehi HD, Random perturbation methods with applications in science and engineering, vol. 150 (Springer Science & Business Media, 2002)
78. Liptser R, Stoyanov J, Stochastics: An International Journal of Probability and Stochastic Processes 32(3-4), 145 (1990)
79. Kurtz T, Applied Stochastic Analysis pp. 186–209 (1992)
80. DasGupta A, Probability for statistics and machine learning: fundamentals and advanced topics (Springer Science & Business Media, 2011)
81. Ghosh M, Mukhopadhyay N, Sen PK, Sequential estimation, vol. 904 (John Wiley & Sons, 2011)
82. Popovic L, McKinley SA, Reed MC, SIAM Journal on Applied Mathematics 71(4), 1531 (2011). DOI 10.1137/090775385. URL http://link.aip.org/link/SMJMAP/v71/i4/p1531/s1
83. Roostalu J, Hentrich C, Bieling P, Telley IA, Schiebel E, Surrey T, Science 332(6025), 94 (2011). DOI 10.1126/science.1199945. URL 10.1126/science.1199945 [PubMed: 21350123]
84. Culver-Hanlon TL, Lex SA, Stephens AD, Quintyne NJ, King SJ, Nature Cell Biology 8(3), 264 (2006). DOI 10.1038/ncb1370. URL 10.1038/ncb1370 [PubMed: 16474384]
85. Hughes J, Shastry S, Hancock WO, Fricks J, Journal of Agricultural, Biological, and Environmental Statistics 18(2), 204 (2013). DOI 10.1007/s13253-013-0131-4. URL 10.1007/s13253-013-0131-4
86. Soppina V, Norris SR, Dizaji AS, Kortus M, Veatch S, Peckham M, Verhey KJ, Proceedings of the National Academy of Sciences 111(15), 5562 (2014). DOI 10.1073/pnas.1400759111. URL 10.1073/pnas.1400759111
87. Beeg J, Klumpp S, Dimova R, Gracia RS, Unger E, Lipowsky R, Biophysical Journal 94(2), 532 (2008). DOI doi: DOI: 10.1529/biophysj.106.097881. URL http://www.sciencedirect.com/science/article/B94RW-4TX32HD-T/2/ef3b41682e7d4db8d3bf0ad83e732363 [PubMed: 17872957]
88. Mirzakhalili E, Nam W, Epureanu BI, Nonlinear Dynamics 90(1), 425 (2017). DOI 10.1007/s11071-017-3673-0. URL 10.1007/s11071-017-3673-0
89. Resnick S, Adventures in stochastic processes (Birkhäuser Boston Inc., Boston, MA, 1992)
90. Serfozo R, Basics of applied stochastic processes (Springer Science & Business Media, 2009)
91. Trybus KM, Current Biology 23(14), R623 (2013). DOI 10.1016/j.cub.2013.06.005. URL http://www.sciencedirect.com/science/article/pii/S0960982213006969 [PubMed: 23885882]
92. Driver JW, Jamison DK, Uppulury K, Rogers AR, Kolomeisky AB, Diehl MR, Biophysical Journal 101(2), 386 (2011). DOI 10.1016/j.bpj.2011.05.067. URL http://www.sciencedirect.com/science/article/pii/S0006349511007004 [PubMed: 21767491]
93. Müller MJ, Klumpp S, Lipowsky R, Biophysical Journal 98(11), 2610 (2010). DOI DOI: 10.1016/j.bpj.2010.02.037. URL http://www.sciencedirect.com/science/article/B94RW-506R4PY-V/2/5ba527d4133e6ca2ae6eca74b4cdbb80 [PubMed: 20513405]
94. Veretennikov AY, Pardoux, The Annals of Probability 31(3), 1166 (2003). DOI 10.1214/aop/1055425774. URL http://projecteuclid.org/euclid.aop/1055425774

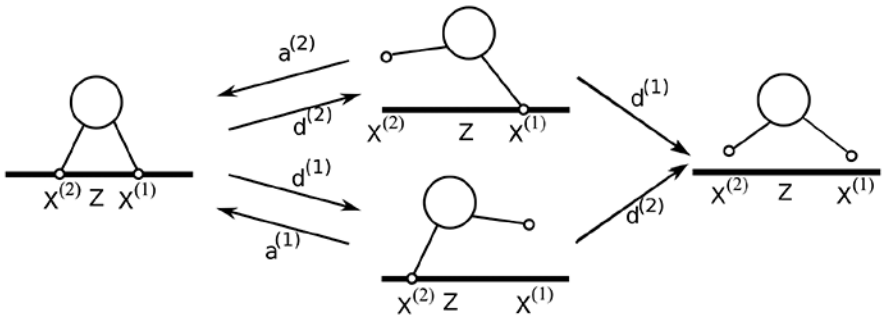

Fig. 1:

Attachment and detachment from a microtubule for a system of two motors durably attached to a cargo. The spatial positions along the microtubule for the motors are denoted $X^{(1)}$, and $X^{(2)}$, and for the cargo by Z. From a state with two attached motors (left), each motor i can detach with a rate $d^{(i)}$ depending on the current spatial configuration. From a state with one attached and one detached motor (center), the detached motor i can (re)attach with a constant rate $a^{(i)}$, or the attached motor i' can also detach at a configuration-dependent rate $d^{(i')}$, terminating the run on the microtubule.

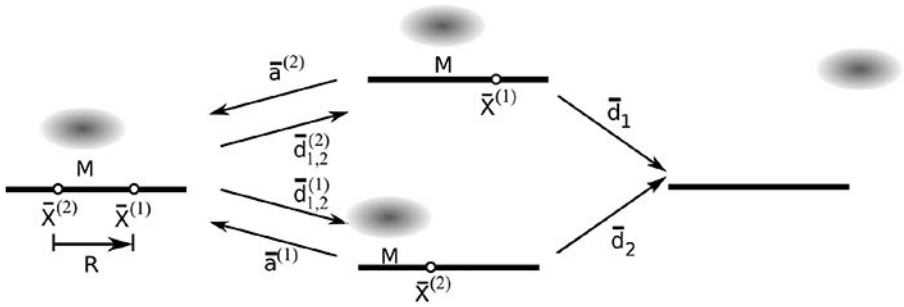

Fig. 2: Switched diffusion model.

Effective dynamics of cargo with two attached motors on time scale $\tilde{a}^{(i)} \sim \tilde{d}^{(i)} \ll \varepsilon^{(i)} \ll \tilde{t} \ll 1 \ll (\Gamma^{(i)})^{-1}$ long compared to detached motor and cargo fluctuation dynamics but short compared to attached motor dynamics. The cargo dynamics are represented on this time scale by a cargo tracking variable M, as discussed in Subsection 4.1. Left: A cargo with both motors attached to the microtubule. The cargo tracking variable dynamics (41) and the detachment rate $\bar{d}^{(i)}_{1,2}$ (44) of each motor i depends on the displacement R between the attached motors, also evolving dynamically. Middle: With only one motor attached, the cargo tracking variable M with one attached motor evolves with constant drift (30) and diffusivity (31). From these states, the system either detaches completely (as shown in the rightmost part of the figure), with effective rate given in (46) or returns to having two attached motors, with rates $\bar{a}^{(i)}$ (47).

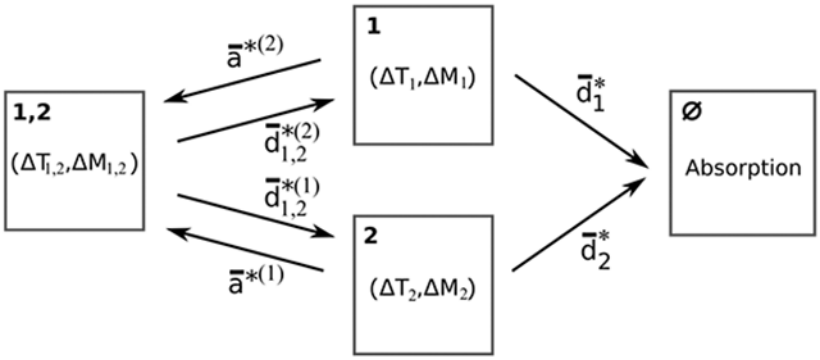

Fig. 3: Coarse-grained Markov chain model.

Under the assumption of slow switching, the switched diffusion model (see Fig. 2) is further coarsened by averaging intermotor separation. The random duration ΔT_{ϖ} spent in state ϖ is exponentially distributed with mean determined in the usual way by the transition rates out the state. The random displacement ΔM_{ϖ} for each attachment state ϖ (shown in the upper left corner of each box) is then found through (27). Detachment rates $\bar{d}_{1,2}^{*(i)}$ from the state of two attached motors, given by (43), are now constants coarse-grained with respect to intermotor separation.

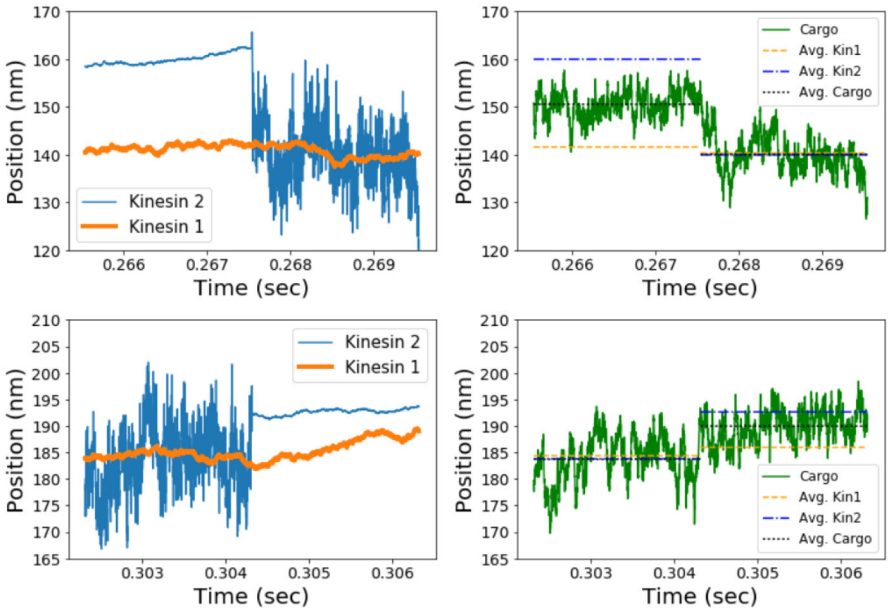

Fig. 4:

Switching behavior for a sample path of the kinesin-1/kinesin-2 complex simulation under trap force $F_T = 0$ using double exponential detachment rate functions and parameters taken from Table 1. Recall that the molecular motor dynamics are approximated via continuous diffusion processes, so the small fluctuations (< 8 nm) of attached motors are a model artifact that are not supposed to affect the central concerns of this work. Top left: Motor behavior at a detachment event, with kinesin-1 (thick orange) attached at all times shown, and kinesin-2 (thin blue) detaching near $t = .2675$ s. Top right: Behavior of cargo during this detachment event. Dashed lines denote numerical averages for positions of motors and cargo taken over .002 seconds before and after detachment. Bottom left: Motor behavior at an attachment event, with kinesin-1 (thick orange) attached at all times shown, and kinesin-2 (thin blue) attaching near $t = .3043$ s. Bottom right: Behavior of cargo during this attachment event. Dashed lines denote numerical averages for positions of motors and cargo taken over .002 seconds before and after attachment.

Table 1:

Typical values for kinesin-1 in water-like environments at saturating ATP concentrations. Values of parameters which differ for kinesin-2 (specifically, KIF3A/B) are in bold with parentheses [69, 32, 18, 34, 16, 14, 17].

Parameter	Description	Typical values
F_s^i	Motor stall force	7 pN [69]
k_BT	Boltzmann constant by temperature	4.1 pN nm
$\kappa^{(i)}$	Motor-cargo tether spring constant	0.25 pN/nm [32]
$v^{(i)}$	Unencumbered motor velocity	790 nm/s (**500 nm/s**) [18]
γ	Cargo friction	1×10^{-5} pN s/nm [34]
$\gamma_{m,i}$	Motor friction	1×10^{-6} pN s/nm
$(\sigma^{(i)})^2$	Effective motor diffusion	5000 nm^2/s (**1500 nm^2/s**)[69, 18]
F_T	Optical trapping force	−20 pN to 6 pN [16]
$d^{(i)}$	Motor attachment rate	4/s (**16/s**) [14]
$d_{0-}^{(i)}$	Small assisting force detachment rate	9.1/s **(5.6/s)** [16, 17]
$d_{0+}^{(i)}$	Small hindering force detachment rate	0.7/s **(2.3/s)** [16, 17]
$F_{d-}^{(i)}$	Assisting force detachment scale	14 pN **(10 pN)** [16, 17]
$F_{d+}^{(i)}$	Hindering force detachment scale	2.1 pN **(2.0 pN)** [16, 17]

Table 2:

Nondimensional groups and typical values for kinesin-1 and kinesin-2. When only a single value is given, it is common to both. Otherwise the kinesin-1 value is listed first, with the kinesin-2 value in bold text in parentheses. Attachment and detachment scales are taken for hindering forces.

Group	Definition	Typical value
$\varepsilon^{(i)}$	$\frac{\boldsymbol{v}^{(i)}\gamma}{\sqrt{2k_BT\overline{\boldsymbol{\kappa}}}}$	6×10^{-3} ($\mathbf{3 \times 10^{-3}}$)
$s^{(i)}$	$\frac{\boldsymbol{\kappa}^{(i)}}{F_s}\sqrt{\frac{2k_BT}{\overline{\boldsymbol{\kappa}}}}$	0.2
$\widetilde{F}_T$	$\frac{F_T}{\sqrt{2k_BT\overline{\boldsymbol{\kappa}}}}$	−10 to 4
$\widehat{\boldsymbol{\rho}}^{(i)}$	$\frac{(\sigma^{(i)})^2\sqrt{\overline{\boldsymbol{\kappa}}}}{\boldsymbol{v}^{(i)}\sqrt{2k_BT}}$	1 (**.5**)
$I^{(i)}$	$\frac{\gamma_m^i}{\gamma}$	0.1
$u^{(i)}$	$\frac{\boldsymbol{\kappa}^{(i)}}{F_d^i}\sqrt{\frac{2k_BT}{\overline{\boldsymbol{\kappa}}}}$	.7 (**.7**)
$\widetilde{a}^{(i)}$	$\frac{a^{(i)}\gamma}{\overline{\boldsymbol{\kappa}}}$	2×10^{-4} ($\mathbf{6 \times 10^{-4}}$)
$\widetilde{d}^{(i)}$	$\frac{d_0^{(i)}\gamma}{\overline{\boldsymbol{\kappa}}}$	3×10^{-5} ($\mathbf{8 \times 10^{-5}}$)

Table 3:
Simulations with constant detachment rate model.

The detachment rates $d^{(i)}(F)$ are taken to be constants obtained by averaging the double exponential detachment rate model (8) against the stationary distribution of the force F when only the motor in question is attached. The columns are organized by applied trap force F_T, with positive (negative) values corresponding to hindering (assisting) forces. The theoretical values are computed according to the formulas from Section 5 while the simulated values are obtained from 2,000 Monte Carlo simulations conducted as described in Section 6. Units of time and distance are measured in seconds and nanometers, respectively. The means of for the number of cycles (including the terminal one) $N_c + 1$, run time T, and run length L are estimated with the sample mean, where intervals denote the standard error. The errors in the ensemble and long-run velocities (V_{ens} and V_{run}) and diffusivities (D_{ens} and D_{run}) are obtained through bootstrap sampling with 1,000 bootstrap samples.

	F_T = −5 pN		F_T = 0 pN		F_T = 5 pN	
	Simulation	**Theory**	**Simulation**	**Theory**	**Simulation**	**Theory**
	kinesin-1/kinesin-1					
V_{run}	951 ± 4	946	758 ± 4	755	257 ± 5	257
V_{ens}	951 ± 3	946	758 ± 2	755	256 ± 3	257
D_{run}	2700 ± 200	2500	2100 ± 200	2100	3900 ± 300	3400
D_{ens}	2500 ± 100	2500	2100 ± 100	2100	3700 ± 200	3400
$\mathbb{E}[N_c + 1]$	1.72 ± .03	1.74	1.73 ± .03	1.74	1.74 ± .03	1.74
$\mathbb{E}[T]$	.34 ± .01	.33	.35 ± .01	.35	.34 ± .01	.35
$\mathbb{E}[L]$	326 ± 6	329	263 ± 5	263	88 ± 2	90
	kinesin 2/kinesin 2					
V_{run}	628 ± 2	632	483 ± 2	482	168 ± 3	174
V_{ens}	630 ± 1	632	483 ± 1	482	171 ± 1	174
D_{run}	900 ± 100	1000	610 ± 60	630	1600 ± 100	1200
D_{ens}	950 ± 40	1000	630 ± 30	620	1350 ± 60	1220
$\mathbb{E}[N_c + 1]$	4.36 ± .08	4.29	4.24 ± .08	4.29	4.40 ± .09	4.29
$\mathbb{E}[T]$	.66 ± .01	.65	.64 ± .01	.65	.67 ± .01	.65
$\mathbb{E}[L]$	411 ± 9	408	311 ± 6	311	114 ± 3	112
	kinesin-1/kinesin-2					
V_{run}	749 ± 6	727	583 ± 4	578	202 ± 5	210
V_{ens}	728 ± 3	688	569 ± 2	554	200 ± 2	198
D_{run}	4000 ± 400	4400	1800 ± 100	2200	2800 ± 300	2200
D_{ens}	3500 ± 200	3700	1800 ± 100	2000	2300 ± 100	2200
$\mathbb{E}[N_c + 1]$	2.36 ± .04	2.45	2.44 ± .04	2.45	2.44 ± .04	2.45
$\mathbb{E}[T]$	.42 ± .01	.42	.44 ± .01	.42	.44 ± .01	.42
$\mathbb{E}[L]$	308 ± 6	305	250 ± 5	242	87 ± 2	88

Table 4:
Simulations with double exponential detachment rate model.

The detachment rates $d^{(i)}(F)$ are given by the double exponential detachment rate model (8). The columns are organized by applied trap force F_T, with positive (negative) values corresponding to hindering (assisting) forces. The theoretical values are computed according to the formulas from Section 5 while the simulated values are obtained from 2000 Monte Carlo simulations conducted as described in Section 6. Units of time and distance are measured in seconds and nanometers, respectively. The means of for the number of cycles (including the terminal one) $N_c + 1$, run time T, and run length L are estimated with the sample mean, where intervals denote the standard error. The errors in the ensemble and long-run velocities (V_{ens} and V_{run}) and diffusivities (D_{ens} and D_{run}) are obtained through bootstrap sampling with 1,000 bootstrap samples.

	F_T = −5 pN		F_T = 0 pN		F_T = 5 pN	
	Simulation	**Theory**	**Simulation**	**Theory**	**Simulation**	**Theory**
	kinesin-1/kinesin-1					
V_{run}	1021 ± 7	1026	780 ± 4	776	291 ± 5	289
V_{ens}	1018 ± 4	1026	785 ± 3	776	296 ± 4	289
D_{run}	2800 ± 200	3000	2300 ± 200	2200	3900 ± 200	3500
D_{ens}	2700 ± 100	3000	2200 ± 100	2200	3700 ± 100	3500
$\mathbb{E}[N_c + 1]$	1.31 ± .01	1.30	1.74 ± .03	1.74	1.45 ± .02	1.44
$\mathbb{E}[T]$	.15 ± .01	.14	.33 ± .01	.32	.30 ± .01	.28
$\mathbb{E}[L]$	148 ± 3	144	262 ± 5	247	88 ± 2	80
	kinesin-2/kinesin-2					
V_{run}	675 ± 3	675	487 ± 2	482	19 ± 8	67
V_{ens}	676 ± 2	675	487 ± 1	482	37 ± 5	67
D_{run}	1300 ± 100	1300	630 ± 60	690	2600 ± 200	1700
D_{ens}	1280 ± 50	1260	650 ± 30	680	2200 ± 100	1600
$\mathbb{E}[N_c + 1]$	2.67 ± .05	2.75	4.40 ± .09	4.28	1.45 ± .02	1.47
$\mathbb{E}[T]$	.29 ± .01	.30	.63 ± .01	.57	.10 ± .01	.10
$\mathbb{E}[L]$	197 ± 4	201	308 ± 7	276	3.6 ± .5	6.7
	kinesin-1/kinesin-2					
V_{run}	812 ± 6	878	615 ± 4	612	196 ± 6	208
V_{ens}	804 ± 4	823	604 ± 2	586	187 ± 4	185
D_{run}	2800 ± 200	5800	2200 ± 200	2600	2600 ± 200	2200
D_{ens}	3100 ± 100	5500	2300 ± 100	2500	2600 ± 100	2300
$\mathbb{E}[N_c + 1]$	1.77 ± .03	1.89	2.81 ± .05	2.73	1.77 ± .02	1.76
$\mathbb{E}[T]$	.21 ± .01	.20	.49 ± .01	.42	.20 ± .01	.20
$\mathbb{E}[L]$	169 ± 3	178	293 ± 6	258	38 ± 1	42